



Study of $Z \rightarrow ll\gamma$ decays at $\sqrt{s} = 8$ TeV with the ATLAS detector

ATLAS Collaboration*

CERN, 1211 Geneva 23, Switzerland

Received: 19 October 2023 / Accepted: 22 January 2024
© CERN for the benefit of The ATLAS Collaboration 2024

Abstract This paper presents a study of $Z \rightarrow ll\gamma$ decays with the ATLAS detector at the Large Hadron Collider. The analysis uses a proton–proton data sample corresponding to an integrated luminosity of 20.2 fb^{-1} collected at a centre-of-mass energy $\sqrt{s} = 8$ TeV. Integrated fiducial cross-sections together with normalised differential fiducial cross-sections, sensitive to the kinematics of final-state QED radiation, are obtained. The results are found to be in agreement with state-of-the-art predictions for final-state QED radiation. First measurements of $Z \rightarrow ll\gamma\gamma$ decays are also reported.

Contents

1	Introduction
2	The ATLAS detector
3	Data and simulated event samples
4	Selection of $Z \rightarrow ll\gamma$ events
4.1	Photon and lepton selection
4.2	Signal region definition
5	Background estimation
6	Correction for detector effects
7	Systematic uncertainties
8	Results for $Z \rightarrow ll\gamma$ process
8.1	Differential cross-sections
8.2	Integrated fiducial cross-sections
9	First measurement of the $Z \rightarrow ll\gamma\gamma$ process
10	Conclusions
	References

1 Introduction

The production of Z bosons and their decay to lepton pairs at the Large Hadron Collider (LHC) through the Drell–Yan mechanism has been a topic of very fruitful and detailed studies in the LHC experiments, and the precision of the measurements has led over the past decade to impressive theoretical

developments, mostly in the area of higher-accuracy quantum chromodynamic (QCD) predictions.

Precise predictions for quantum electrodynamic and electroweak (QED/EW) effects are also of prime importance for key measurements at the LHC, such as that of the W -boson mass or of the weak mixing angle; this became very clear already at the end of the Run-1 data-taking period [1]. The analysis described in this paper focuses on the final-state radiation of photons in Drell–Yan production of Z bosons decaying to an electron or muon pair. This process, denoted in the following as QED FSR (Fig. 1), can be calculated separately from QED initial-state radiation or QED ISR (Fig. 2) and from initial-final-state interference (IFI) thanks to gauge invariance. Owing both to the kinematic selections applied to the final state particles, and to the narrow width of the Z boson, the contributions from QED ISR and QED IFI in the fiducial phase space of the measurements described below are expected to be very small [2].

When considering QED radiation, fixed-order partitioning of the calculations has been shown at the time of the Large Electron-Positron Collider (LEP) to be sub-optimal in terms of obtaining the most precise predictions.

Photon resummation techniques using exponentiation were originally developed by Yennie–Frautschi–Suura (YFS) [3] for inclusive QED FSR in the case of e^+e^- collisions. They were then expanded to be used for exclusive QED ISR and FSR and for pp collisions at the LHC [2]. This analysis uses and compares several state-of-the-art implementations, namely KKMChh [4–6], Sherpa [7, 8], and Photos [9]. In the latter case, which applies only to QED FSR, Photos is used within Powheg+Pythia [10–14], as described in Sect. 3. These Monte-Carlo (MC) tools provide complete simulated events at LHC energies, in which the final state frequently contains several soft/collinear photons near the final-state leptons from the Z -boson decay, in addition to the single hard large-angle photon emission required by the analysis selection described in Sect. 4. The YFS approach resides on the idea of resumming the leading soft logarithms to all orders, rather than focusing on the leading collinear terms. These

* e-mail: atlas.publications@cern.ch

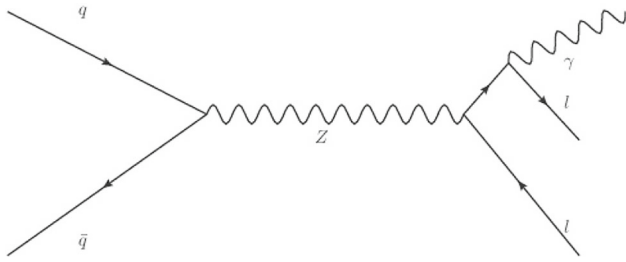


Fig. 1 Example of $q\bar{q} \rightarrow Z \rightarrow ll\gamma$ final-state QED radiation diagram

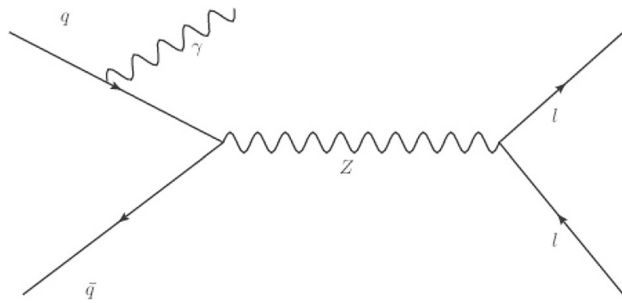


Fig. 2 Example of $q\bar{q} \rightarrow Z \rightarrow ll\gamma$ initial-state QED radiation diagram

soft logarithms are largely independent of the inner process characteristics and can be calculated from the external particles and their four-momenta only. The big advantage of the YFS formalism is that in addition it allows for a systematic improvement of this eikonal approximation, order-by-order in the QED coupling constant [15, 16]. As discussed in Sect. 8, the measurement results presented in this paper cover normalised fiducial differential cross-sections and fiducial integrated cross-sections for $Z \rightarrow ll\gamma$ decays and a first measurement of $Z \rightarrow ll\gamma\gamma$ decays.

One often labels the leptons in such final-state configurations as “bare” leptons, a notation adopted throughout this paper, even though the meaning of such a bare lepton is by definition dependent on the tool used to describe multiple-photon emissions in QED FSR. One can also define a “dressed” lepton by combining the bare four-momenta of each lepton with that of QED FSR photons collected close to the lepton within a cone of size $\Delta R = 0.1$ around it.

Since soft/collinear QED emissions are regularised by the lepton mass, the predictions for the kinematic observables describing the final state will differ significantly in some regions of phase space between bare electrons and bare muons when considering the calculations using exponentiation described above. This is shown in the case of predictions from Sherpa 2.2.4 [8] in Fig. 3 for the shape of the normalised distribution for the invariant mass, $m_{l+\gamma}$, of the positively charged lepton and the photon and for the angular separation, $\Delta R_{l\gamma}$, between the photon and the closer of the two leptons. For large values of $m_{l+\gamma}$, which are close to the

edge of the phase space available for $Z \rightarrow ll\gamma$ decays, and for large values of $\Delta R_{l\gamma}$, which correspond to specific configurations of $Z \rightarrow ll\gamma$ decays where the dilepton pair and the photon are back-to-back, Fig. 3 shows that one expects about 5% fewer $Z \rightarrow ee\gamma$ decays than $Z \rightarrow \mu\mu\gamma$ decays relative to the bulk of the distribution. It should be noted that most of the difference between electrons and muons observed in these plots for the bulk of the distributions is due to the higher acceptance in η for the muons (see Table 2).

Fig. 3 also shows that the dressed lepton definition minimises the differences between electrons and muons. The use of dressed leptons also minimises the impact of the QED FSR radiation on the integrated cross-sections. It is often used for exclusive analyses of e.g. Z/W +jet production because it unambiguously assigns the QED FSR photons to the leptons rather than to hadronic jets when performing such exclusive measurements. However, it is not optimal for precise studies of the QED FSR radiation itself.

For the purpose of the analysis described in this paper, all results presented in Sect. 8 are shown separately for bare electrons and muons with the exception of the low-statistics measurement of $Z \rightarrow ll\gamma\gamma$ final states described in Sect. 9, in which bare electrons and muons are combined. However, all the dressed-lepton results are published in HEPDATA as well. The measured normalised differential distributions of the invariant mass of the negatively charged lepton and the photon are also published in HEPDATA, together with the charge asymmetry distribution and the full covariance matrix describing the uncertainties in all these measurements with their correlations.

2 The ATLAS detector

The ATLAS experiment [17] at the LHC is a multipurpose particle detector with a forward–backward symmetric cylindrical geometry and a near 4π coverage in solid angle.¹ It consists of an inner tracking detector surrounded by a thin superconducting solenoid providing a 2 T axial magnetic field, electromagnetic and hadron calorimeters, and a muon spectrometer. The inner tracking detector covers the pseudorapidity range $|\eta| < 2.5$. It consists of silicon pixel, silicon microstrip, and transition radiation tracking detectors. Lead/liquid-argon (LAr) sampling calorimeters provide electromagnetic (EM) energy measurements with high gran-

¹ ATLAS uses a right-handed coordinate system with its origin at the nominal interaction point (IP) in the centre of the detector and the z -axis along the beam pipe. The x -axis points from the IP to the centre of the LHC ring, and the y -axis points upwards. Cylindrical coordinates (R, ϕ) are used in the transverse plane, ϕ being the azimuthal angle around the z -axis. The pseudorapidity is defined in terms of the polar angle θ as $\eta = -\ln \tan(\theta/2)$. Angular distance is measured in units of $\Delta R \equiv \sqrt{(\Delta\eta)^2 + (\Delta\phi)^2}$.

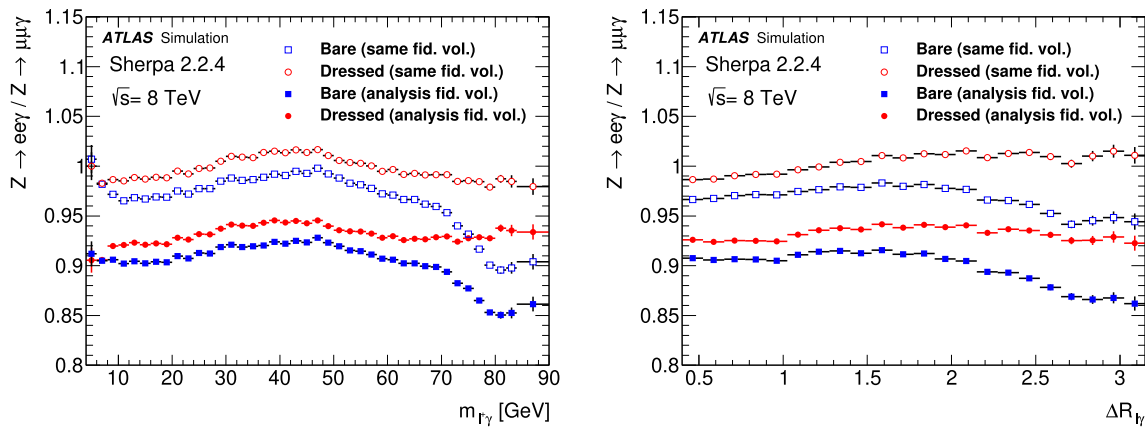


Fig. 3 Predicted ratios of expected differential cross-sections for the invariant mass, $m_{l\gamma}$, of the positively charged lepton and the photon (left) and of the angular separation, $\Delta R_{l\gamma}$, between the photon and the closer of the two leptons (right) for electrons compared to muons. The ratios are shown for the bare and dressed lepton definitions described in the text. The predictions are obtained from a high-statistics inclusive Z -boson sample using Sherpa 2.2.4 and are shown for events contain-

ing two high- p_T leptons and one high- p_T photon satisfying the fiducial volume selections described in Table 2 in Sect. 6 (full symbols). Since most of the difference between electrons and muons observed in this case for the bulk of the distributions is due to the higher acceptance in η for the muons, the electron to muon ratios are also shown in the case of identical fiducial selections for both charged leptons (open symbols)

ularity. A steel/scintillator-tile hadronic calorimeter covers the central pseudorapidity range ($|\eta| < 1.7$). The end-cap and forward regions are instrumented with LAr calorimeters for both the EM and hadronic energy measurements up to $|\eta| = 4.9$. The muon spectrometer surrounds the calorimeters and is based on three large superconducting air-core toroidal magnets with eight coils each. The field integral of the toroids ranges between 2.0 and 6.0 Tm across most of the detector. The muon spectrometer includes a system of precision tracking chambers and fast detectors for triggering. A three-level trigger system is used to select events to be recorded. The first-level trigger is implemented in hardware and uses a subset of the detector information to accept events at a rate of at most 75 kHz. This is followed by two software-based trigger levels that together reduce the accepted event rate to 400 Hz on average depending on the data-taking conditions during 2012. An extensive software suite [18] is used in the reconstruction and analysis of real and simulated data, in detector operations, and in the trigger and data acquisition systems of the experiment.

3 Data and simulated event samples

The data used in this analysis was collected in 2012 using pp collisions at a centre-of-mass energy of 8 TeV. The corresponding total integrated luminosity is $20.2 \pm 0.4 \text{ fb}^{-1}$. The average number of inelastic pp interactions produced per bunch crossing for this dataset is 20.7.

The PowhegBox v1 MC programme [10–13] was used for the simulation of Z -boson decays at next-to-leading

order (NLO) in QCD using the CTEQ6L1 PDF set [19]. It was interfaced to Pythia8 [14] for the modelling of the parton shower, hadronisation, and underlying event, with parameters set according to the AU2 CT10 tune [20]. QED FSR is modelled using the exponentiated multi-photon emission provided by Photos [21]. This combination of MC tools, denoted Powheg+Pythia8+Photos, is used as the main MC sample to estimate the effects of detector efficiency and resolution and to unfold the data presented in this paper. Initial-state radiation of photons (QED ISR) and initial-final-state interference (IFI) are not included in the simulation. For QED FSR photons, Photos is configured to include a matrix-element correction for Z -boson decay which brings it very close in accuracy (better than 10^{-3}) to NNLO QED [9] for the emission of up to two photons.

An alternative prediction for $pp \rightarrow ll\gamma$ production with up to three additional parton emissions at leading order in the strong coupling is provided by Sherpa 1.4.1 [7] using the CT10 PDF set [22]. Sherpa 1.4.1 is configured such that the leading photon is generated at matrix-element level with leading-order accuracy. Both FSR and ISR emissions, but not the small effects expected from IFI, are included in the simulation. The YFS [3] approach is then used to exponentiate the radiation in a way similar to that done in Photos. The results obtained by using Sherpa 1.4.1 are compared to those obtained by using Powheg+Pythia8+Photos for a cross-check of the systematics related to the unfolding procedure. A specific version of Sherpa 1.4 (labelled Sherpa 1.4 ME $_{\gamma\gamma}$) containing an exact description at tree level of the production of lepton pairs accompanied by two hard photons has

order (NLO) in QCD using the CTEQ6L1 PDF set [19]. It was interfaced to Pythia8 [14] for the modelling of the parton shower, hadronisation, and underlying event, with parameters set according to the AU2 CT10 tune [20]. QED FSR is modelled using the exponentiated multi-photon emission provided by Photos [21]. This combination of MC tools, denoted Powheg+Pythia8+Photos, is used as the main MC sample to estimate the effects of detector efficiency and resolution and to unfold the data presented in this paper. Initial-state radiation of photons (QED ISR) and initial-final-state interference (IFI) are not included in the simulation. For QED FSR photons, Photos is configured to include a matrix-element correction for Z -boson decay which brings it very close in accuracy (better than 10^{-3}) to NNLO QED [9] for the emission of up to two photons.

An alternative prediction for $pp \rightarrow ll\gamma$ production with up to three additional parton emissions at leading order in the strong coupling is provided by Sherpa 1.4.1 [7] using the CT10 PDF set [22]. Sherpa 1.4.1 is configured such that the leading photon is generated at matrix-element level with leading-order accuracy. Both FSR and ISR emissions, but not the small effects expected from IFI, are included in the simulation. The YFS [3] approach is then used to exponentiate the radiation in a way similar to that done in Photos. The results obtained by using Sherpa 1.4.1 are compared to those obtained by using Powheg+Pythia8+Photos for a cross-check of the systematics related to the unfolding procedure. A specific version of Sherpa 1.4 (labelled Sherpa 1.4 ME $_{\gamma\gamma}$) containing an exact description at tree level of the production of lepton pairs accompanied by two hard photons has

also been used to compare its predictions to the unfolded $Z \rightarrow ll\gamma\gamma$ measurements.

For the comparisons between predictions and the unfolded data, additional generator-level predictions for $pp \rightarrow ll\gamma$ and $pp \rightarrow ll\gamma\gamma$ production have been produced using Sherpa 2.2.4 [8] and KKMChh [5,6]. The QED treatment in Sherpa 2.2.4 is identical to that described above for Sherpa 1.4.1, while the QCD treatment is more advanced [23]. KKMChh is an event generator for Z boson production and decays, that includes exponentiated multi-photon initial and final state radiation and virtual electroweak corrections. It separates the expected dominant contribution from QED FSR to the measurements presented in this paper from the negligible contributions from QED ISR and QED IFI.

To minimise the impact of differences in the QCD aspects on the measurements of QED FSR differential spectra, the MC predictions for which data and MC are not expected to agree to better than 0.5% should be reweighted to the data. This procedure was applied for the p_T^Z spectrum, which is only predicted at leading order in QCD for the two main MC samples used in the analysis. Other distributions have also been studied to assess the residual systematic uncertainties from the QCD aspects of the simulation in the measurements. This reweighting procedure is also applied to the MC predictions at generator level from Sherpa 2.2.4 and from KKMC-hh.

Background contributions from top-quark production ($t\bar{t}$, Wt , and t -channel single top production) are generated using PowhegBox with the CT10 PDF in conjunction with Pythia6 [24] (v6.427 using the CTEQ6L1 PDF) with the Perugia 2011C tune for parton showering, hadronisation, and underlying event. Background contributions from Z+jet and $Z \rightarrow \tau\tau$ production have been simulated using Sherpa 1.4.3 [7] with its default tune and the CT10 PDFs.

The MC samples were processed through a full ATLAS detector simulation [25], based on GEANT4 [26], and reconstructed with the same software as that used for the data. All MC samples are corrected with data-driven factors to account for small differences in photon and lepton trigger, reconstruction, identification and isolation efficiencies between data and simulation. Additional $p-p$ interactions (pile-up), occurring in the same and neighbouring bunch crossings are simulated and overlaid at the detector hit level on top of the hard-scattering process from the MC simulation.

4 Selection of $Z \rightarrow ll\gamma$ events

A $Z \rightarrow ll\gamma$ candidate is formed by selecting the opposite-sign same-flavour dilepton pair with mass closest to m_Z and the highest p_T photon in the event. No explicit requirements are made on the presence or absence of other activity in the event, such as additional photons or leptons or jets. Only

prompt leptons/photons are considered for the signal, meaning that they should not originate from decays of hadrons or τ -leptons. Background events from processes producing fake or non-prompt photons/leptons are suppressed by the lepton/photon identification criteria described below, including in particular isolation requirements on both leptons and on the photon.

Event candidates in both data and MC simulation are required to have fired at least one unprescaled single lepton or dilepton trigger, with a lowest p_T threshold of 24 GeV for single leptons and of 12–13 GeV for dilepton triggers. The single lepton triggers provide a high trigger efficiency with respect to the offline selection, which requires at least one lepton with $p_T > 25$ GeV. The trigger efficiency for $Z \rightarrow ll\gamma$ events satisfying all the selection criteria described below is about 99%.

4.1 Photon and lepton selection

Photon and electron candidates are reconstructed [27] from clusters of energy deposits in the electromagnetic calorimeter combined with information from charged tracks reconstructed in the inner detector. Electrons and photons are identified by shower shape and hadronic leakage variables. Photons are required to satisfy all the requirements on shower-shape variables corresponding to the *Tight* photon identification criteria of Ref. [28]. Electron candidates are required to satisfy the *Loose* likelihood requirement of Ref. [29].

Photon (electron) candidates are required to have a transverse momentum above 15 GeV (10 GeV) and a pseudorapidity in the range $|\eta| < 2.37$ ($|\eta| < 2.47$). For the photon candidates, the transition region between the barrel and end-cap electromagnetic calorimeters, $1.37 < |\eta| < 1.52$, is excluded.

Muon candidates are reconstructed [30] from combined tracks in the inner detector and muon spectrometer with a transverse momentum above 10 GeV over the pseudorapidity range $|\eta| < 2.5$. Over the range $2.5 < |\eta| < 2.7$, stand-alone muon candidates in the muon spectrometer are used, based on tracks with reconstructed segments in three spectrometer stations.

Electron and muon candidates are required to originate from the appropriate primary vertex (each primary vertex candidate is reconstructed from at least two associated tracks with $p_T > 0.4$ GeV). The significance of the transverse impact parameter, defined as the absolute value of the track transverse impact parameter, d_0 , measured relative to the beam trajectory, divided by its uncertainty, σ_{d_0} , must satisfy $|d_0|/\sigma_{d_0} < 5$ for electrons and $|d_0|/\sigma_{d_0} < 3$ for muons. The longitudinal impact parameter is required to satisfy $|z_0| < 10$ mm.

The photon, electron, and muon candidates are required to be isolated from other particles using selections based on calorimeter isolation, which is defined as the sum of the

calorimeter cell transverse energies, $\sum E_T$, inside an isolation cone of $\Delta R = 0.2$ around the lepton or photon [31]. In the case of the calorimeter isolation for photons/electrons, the cells corresponding to the calorimeter cluster itself are excluded from the sum. In addition, the calorimeter isolation is corrected on an event-by-event basis for the energy deposited by the photon or lepton candidate, and, using the method described in Refs. [32–34], for the contribution from the underlying event and pile-up. Each photon/electron (muon) is required to have a normalised calorimeter isolation smaller than 0.3 (0.2). Finally, photons close to leptons are excluded if $\Delta R_{l\gamma} < 0.4$.

4.2 Signal region definition

Candidate $Z \rightarrow ll\gamma$ signal events are selected by requiring that they contain at least one pair of opposite-charge, same-flavour leptons and at least one photon. The highest- p_T lepton is required to have $p_T > 25$ GeV, while the second lepton must have $p_T > 10$ GeV. The selected dilepton pair in the event is that which has an invariant mass, $m_{ll\gamma}$, closest to m_Z . Only 2% of the events have more than one dilepton pair.

To further improve the purity of the QED FSR sample, the invariant mass of the dilepton pair, m_{ll} , is required to be between 20 and 80 GeV, while the three-body invariant mass, $m_{ll\gamma}$, is required to be between 80 and 100 GeV. These selections mainly suppress the background from Z -boson+jet production with a jet misidentified as a photon, which can be clearly seen in Fig. 4 outside the signal region. For similar reasons, these selections also reduce considerably the background from QED ISR. The integrated fiducial cross-section results are also extracted for a stricter selection on the invariant mass of the dilepton, $m_{ll} > 45$ GeV.

The criteria described above were applied to the data, leading to 30571 (resp. 34948) events selected in the $Z \rightarrow ee\gamma$ (resp. $Z \rightarrow \mu\mu\gamma$) channel (see Table 1 and Sect. 5 for more details). The reconstructed differential distributions are shown in Fig. 5 for the three observables of interest, the invariant mass of the positively charged lepton and the photon, $m_{l+\gamma}$, the angular separation between the photon and the closer of the two leptons, $\Delta R_{l\gamma}$, and the transverse momentum of the photon, p_T^γ .

5 Background estimation

The dominant sources of background to the $Z \rightarrow ll\gamma$ signal originate from top-quark pair production and decay with two high- p_T prompt leptons and one prompt photon in the final state and from Z +jet production with two high- p_T prompt leptons and one jet misidentified as a photon in the final state. Other smaller sources of background are also considered, such as $WZ\gamma$ production, $\tau\tau\gamma$ production with two

leptonic decays of the τ -lepton, but also backgrounds with one fake or non-prompt lepton such as $W\gamma$ +jet production and backgrounds from WZ production with the electron from the W -boson decay misidentified as a photon. The sum of all sources contributing to events containing two prompt leptons and one prompt photon is labelled “prompt background” and is predicted by simulation, while the sum of all other sources is labelled “fake γ background” and is estimated from data as described below. The respective contributions of these prompt and fake γ background sources to the data are listed separately with their total uncertainties for the dielectron and dimuon case in Table 1.

The overall background contribution to the signal is expected to be small, as can be seen from the small tails outside the pole region in the three-body invariant mass, $m_{ll\gamma}$, distribution of Fig. 4. A simple extrapolation from the events with large $m_{ll\gamma}$ to the signal region leads to an expectation at the percent level. The nominal method used for the background estimation in this analysis is an unbinned maximum likelihood fit of the $m_{ll\gamma}$ distribution over a wide range, $60 < m_{ll\gamma} < 120$ GeV, using simulation for the prompt background sources (shape and normalisation) and also for the shape of the fake γ background. This fit is performed for each bin of the differential cross-section measurements.

A cross-check of the fake γ background estimate is performed with a data-driven two-dimensional sideband method using an inverted isolation selection for the photon candidate on one side and requiring that $100 < m_{ll\gamma} < 150$ GeV on the other. This latter selection enhances the fake γ background (see Fig. 4 (top)). The difference between the two methods is used as an estimate of the systematic uncertainty in the fake γ background estimate. As shown in Table 1, the overall background is at the level of 2–3% of the expected signal with a total relative uncertainty of 13%.

6 Correction for detector effects

The reconstructed differential distributions presented in Fig. 5 are corrected for detector effects and bin-to-bin migrations using an iterative Bayesian unfolding method applied to events that pass the detector-level selections. The method is applied with three iterations implemented in the RooUnfold framework [35]. The resulting unfolded distributions for the $Z \rightarrow ee\gamma$ and $Z \rightarrow \mu\mu\gamma$ signal are obtained at both bare-lepton and dressed-lepton level.

The particle-level selections shown in Table 2 are chosen to be as close as possible to the selections described in Sect. 4. The leptons and the photon are required to be prompt, meaning that they should not originate from decays of hadrons or τ -leptons. The small difference in pseudorapidity ranges for electrons and muons is retained at particle level since the

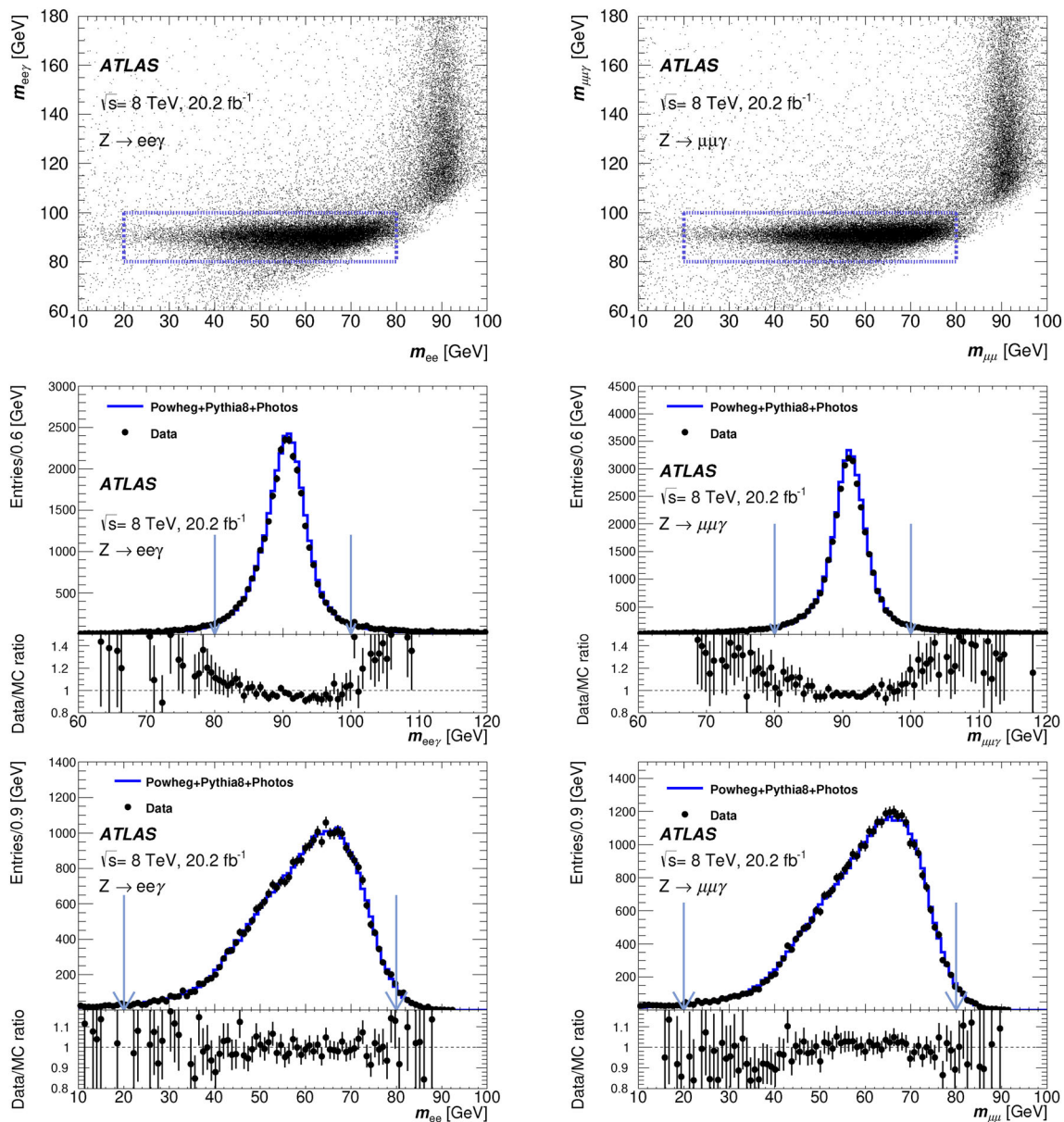


Fig. 4 For $Z \rightarrow ee\gamma$ (left) and $Z \rightarrow \mu\mu\gamma$ (right) decay candidates in data, distribution of the three-body invariant mass, $m_{ll\gamma}$, versus the dilepton mass, m_{ll} . The dashed lines indicate the selection criteria applied in the analysis to these two reconstructed invariant masses. These criteria minimise in particular the background from Z bosons produced in association with jets in which one jet is misiden-

tified as a photon. Also shown are the projections of these figures onto the vertical (middle plot with only the selection on m_{ll} applied) and horizontal (bottom plot with only the selection on $m_{ll\gamma}$ applied) axes with the corresponding vertical lines indicating the selection cuts described above. The curves show the signal predictions from the nominal Powheg+Pythia8+Photos MC normalised to the data

electron and muon channels are not combined in this analysis (except for the low statistics $Z \rightarrow ll\gamma\gamma$ sample described in Sect. 9).

The response matrices, which connect the distributions at reconstruction and particle level, as well as the efficiency correction factors are derived using the Powheg+Pythia+Photos signal MC sample. The reconstruction, trigger and isolation efficiencies as well as the photon/lepton momentum scale and

resolution in the MC simulation are corrected to match those determined in data. The transverse momentum distribution of the simulated $Z \rightarrow ll\gamma$ events was reweighted to that observed in data to minimise the only potentially significant bias from QCD modelling in the simulation (see Sect. 7 for more details). Since the charged leptons and the photon are precisely measured compared to the bin sizes chosen for the

Table 1 Total observed rates of data selected for the measurements in the $Z \rightarrow ee\gamma$ and $Z \rightarrow \mu\mu\gamma$ channels. Also shown are the expected contributions with their total uncertainties from the two main sources of background, the prompt background containing two leptons and one photon, predominantly from top-quark pair production, and the fake γ background containing two leptons and one jet misidentified as a photon, predominantly from Z +jet production (see text). The last row shows the expected signal with its total uncertainty (see Sect. 8.2)

Channel	$Z \rightarrow ee\gamma$	$Z \rightarrow \mu\mu\gamma$
Data	30571	34948
Prompt background	360 ± 40	290 ± 50
Fake γ background	450 ± 90	500 ± 90
Total background	810 ± 100	790 ± 100
$Z \rightarrow ll\gamma$ expected signal	28990 ± 990	34530 ± 1100

differential distributions, the systematic uncertainties related to the unfolding method were found to be below 0.1%.

7 Systematic uncertainties

This section describes the systematic uncertainties in the measurements of the normalised differential fiducial cross-sections for the observables presented in Fig. 5. These systematic uncertainties are grouped according to their source, and their typical relative values over most of the kinematic range of the measured observables are listed in Table 3, while the relative variations of the overall systematic uncertainty as a function of the measured observables are shown in Fig. 6,

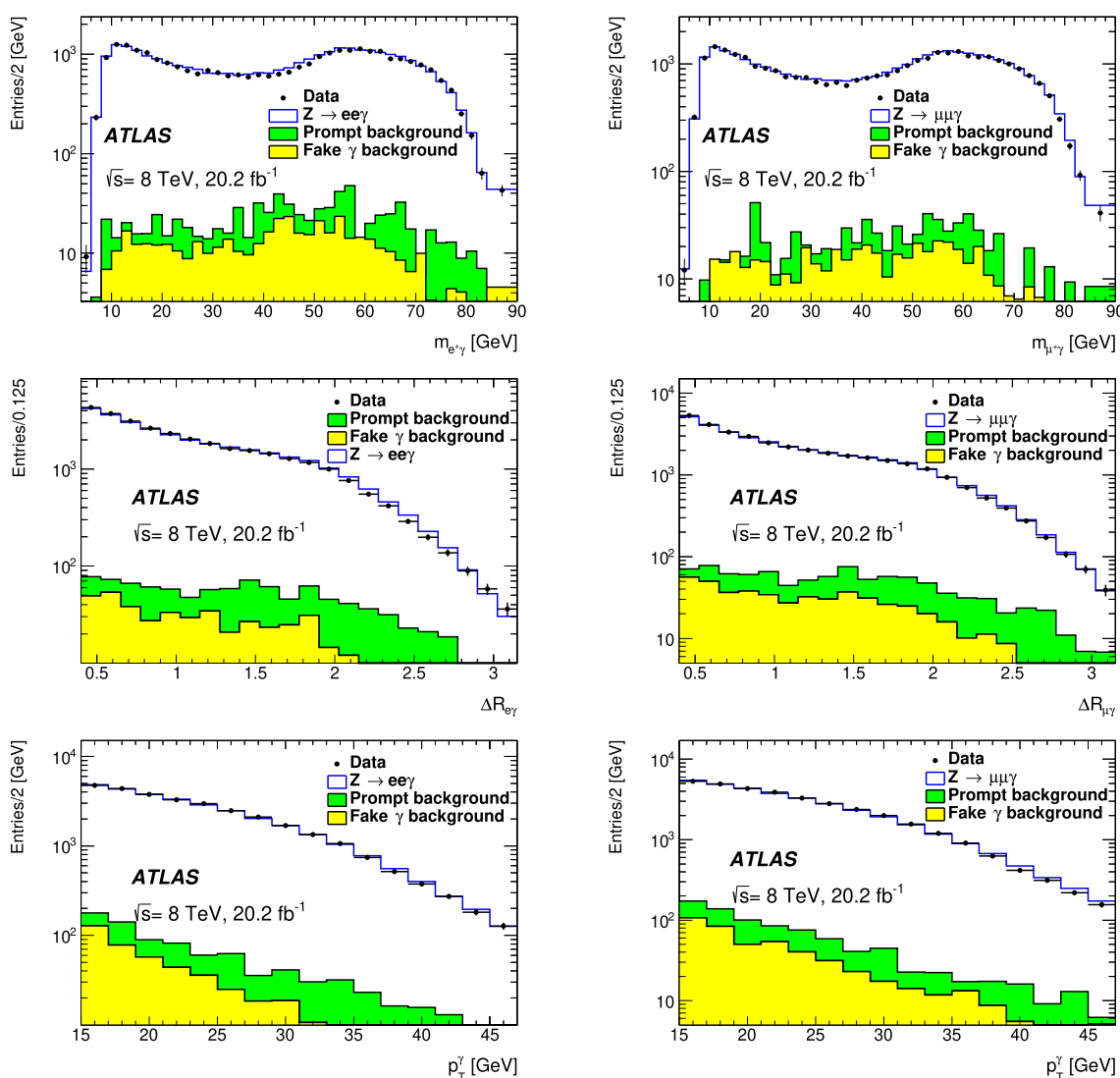


Fig. 5 For electrons (left) and muons (right), measured differential rates for $m_{l+\gamma}$ (top), $\Delta R_{l\gamma}$ (middle), and p_T^γ (bottom). The data are shown compared to the sum of the expected contributions from the $Z \rightarrow ll\gamma$ signal, as predicted from Powheg+Pythia8+Photos, and of the prompt and fake γ backgrounds

Table 2 Fiducial volume selections for $Z \rightarrow ll\gamma$ events

Photon with $p_T > 15$ GeV
$ \eta_\gamma < 2.37$ excluding $1.37 < \eta_\gamma < 1.52$
Leptons with $p_T > 25, 10$ GeV
$ \eta_\mu < 2.7$
$ \eta_e < 2.47$
At least one photon + one pair of same-flavour opposite-sign leptons
$\Delta R_{l\gamma} > 0.4$
$20 < m_{ll} < 80$ GeV
$80 < m_{ll\gamma} < 100$ GeV

together with the variations of the statistical uncertainty in the data and of the total uncertainty in the measurements. The statistical uncertainty in the data is the dominant uncertainty over most of the measurement bins of all three observables.

The experimental systematic uncertainties in measured observables involving only leptons and photons are expected to be small, and particularly so for normalised distributions for which only the shape variations in these uncertainties remain. This can indeed be seen from Table 3 which shows contributions of at most a few per mille from the lepton/photon experimental systematic uncertainty sources. However, Fig. 6 shows that the overall systematic uncertainty is the dominant contribution at the edge of the phase space for the $m_{l+\gamma}$ and $\Delta R_{l\gamma}$ distributions. This arises from the very limited number of simulated events in these regions which inflates the overall systematic uncertainty even though it is statistical in nature.

Over most of the phase space of interest, one expects that the shapes of the electron and muon channels are identical, so the $e - \mu$ difference has been used as an additional cross-check of the experimental systematic uncertainties. The weighted mean of the $e - \mu$ data/MC double ratio difference was found to be -0.0011 ± 0.0085 (stat) ± 0.00007 (syst). The systematic uncertainty is reduced here purely to the contribution of the experimental systematic uncertainties which are uncorrelated between electrons and muons. The $e - \mu$ difference was thus found to be consistent with its statistical uncertainty, and no systematic trend was observed as a function of the measured differential distributions.

Table 3 shows that the theoretical uncertainties from QCD scale variations and PDFs, related to the acceptance of the photon/lepton fiducial cuts, are very small, at the per mille level, as expected. However, any QCD-related mis-modelling of Z -boson production not covered by these uncertainties may have a significant and direct impact on the QED-related observables of interest. As mentioned above, the simulated events were reweighted to reproduce the observed transverse momentum spectrum of $Z \rightarrow ll\gamma$ decays. This has potentially a direct impact on the photon transverse momentum

Table 3 Breakdown of systematic uncertainties for the normalised differential fiducial cross-sections. The values shown are typical over most of the kinematic range of the unfolded observables

Uncertainty source	$Z \rightarrow ee\gamma$ channel (%)	$Z \rightarrow \mu\mu\gamma$ channel (%)
Experimental		
Energy/momentum scale and resolution	0.2	0.2
Efficiency	0.3	0.3
Unfolding	< 0.1	< 0.1
Background subtraction	0.3	0.3
Theory		
PDF	< 0.1	< 0.1
QCD scale variations	0.1	0.1
QCD modelling	0.3	0.3
Total	0.6	0.6

spectrum, but it also affects at the percent level certain regions of phase space for the $m_{l+\gamma}$ and $\Delta R_{l\gamma}$ distributions (the most significant impact has been observed in the case of the Sherpa 1.4 predictions). After this reweighting procedure, the residual QCD modelling systematic uncertainties were found to be very small, at the few per mille level. This was further verified by also reweighting to data the other kinematic observables related to Z -boson production, namely the Z -boson rapidity and the angular coefficients [36] related to the lepton kinematics in the rest-frame of the Z -boson. As a final cross-check, the Sherpa 1.4 predictions for the reconstructed observables, after reweighting to the observed transverse momentum spectrum of $Z \rightarrow ll\gamma$ decays, were unfolded using the nominal Powheg+Pythia+Photos MC. The resulting systematic uncertainty, as derived from the difference between the generator-level Sherpa 1.4 prediction and that obtained after this unfolding cross-check, was found to be negligible, i.e. below the per mille level.

8 Results for $Z \rightarrow ll\gamma$ process

8.1 Differential cross-sections

The measurement results are presented here as unfolded normalised differential cross-sections for the three observables of interest, namely the invariant mass of the positively charged lepton and the photon, $m_{l+\gamma}$, the angular dis-

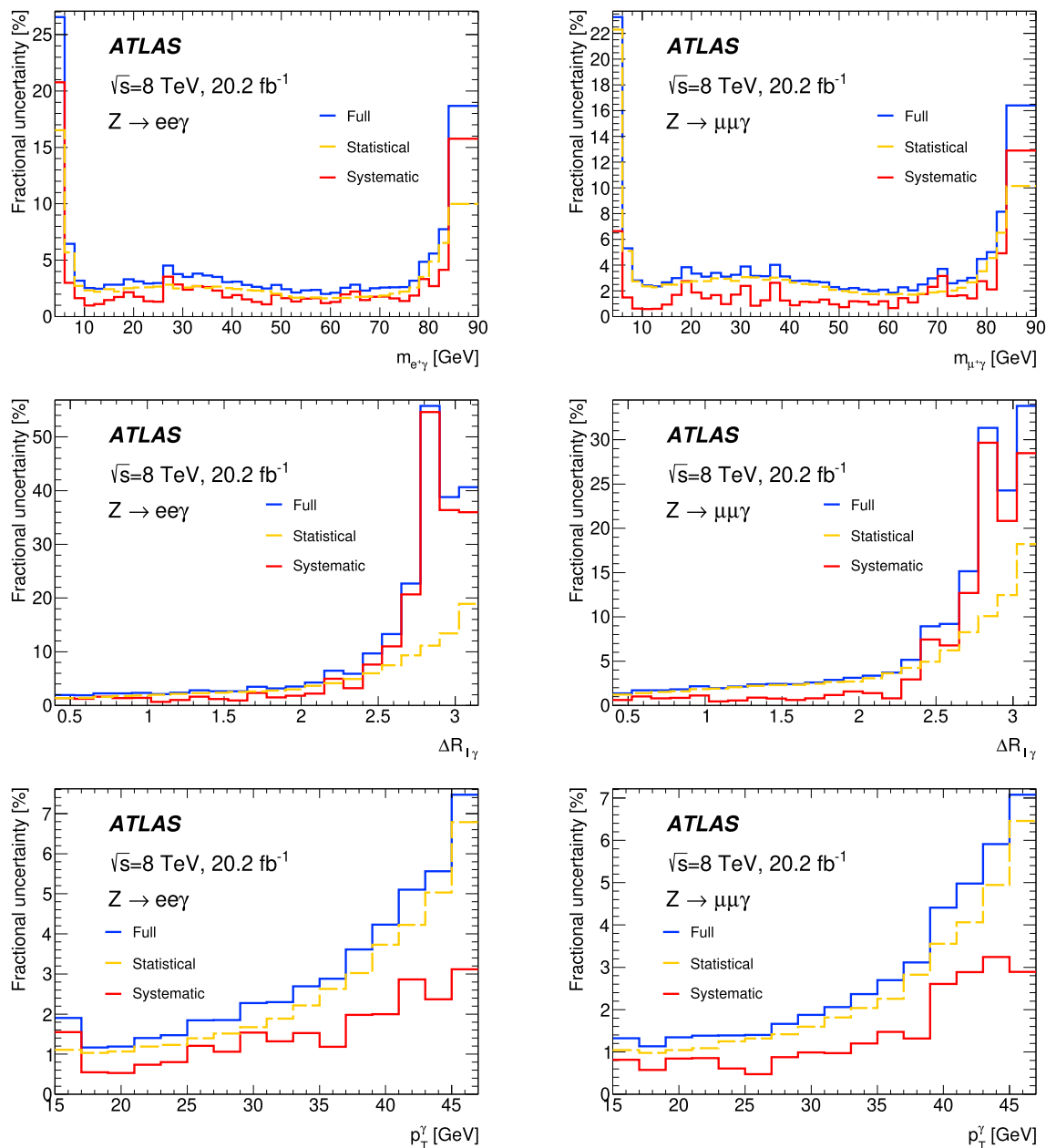


Fig. 6 Breakdown of relative uncertainties for the normalised unfolded differential cross-sections as a function of the observables of interest, $m_{l+\gamma}$ (top), $\Delta R_{l\gamma}$ (middle), and p_T^γ (bottom), shown separately for the $Z \rightarrow ee\gamma$ (left) and $Z \rightarrow \mu\mu\gamma$ (right) channels

tance, $\Delta R_{l\gamma}$, between the photon and the closer of the two leptons, and the transverse momentum, p_T^γ , of the photon. These differential cross-sections are normalised to the total measured fiducial cross-section to minimise the experimental uncertainties and also to remove potentially dominant QCD-related theoretical uncertainties when comparing to predictions. The results below are shown separately for the electron and muon channels in the case of bare leptons. This maximises the sensitivity to expected small differences in the distributions between the two lepton flavours (see Fig. 3).

Fig. 7 shows in the case of bare leptons, separately for the electron and muon channels, the unfolded normalised differential distributions for the data with their uncertainties compared to the predictions with uncertainties from Powheg+Pythia8+Photos, Sherpa 2.2.4 (YFS), and KKM-Chh. As discussed in Sect. 3, Powheg+Pythia8+Photos considers only QED FSR and has an associated theoretical uncertainty of 0.2% obtained by varying the configuration of Photos from its default one to the slightly less precise prediction not including the Z -boson matrix-element correction discussed in Sect. 3. This small theoretical uncertainty assumes

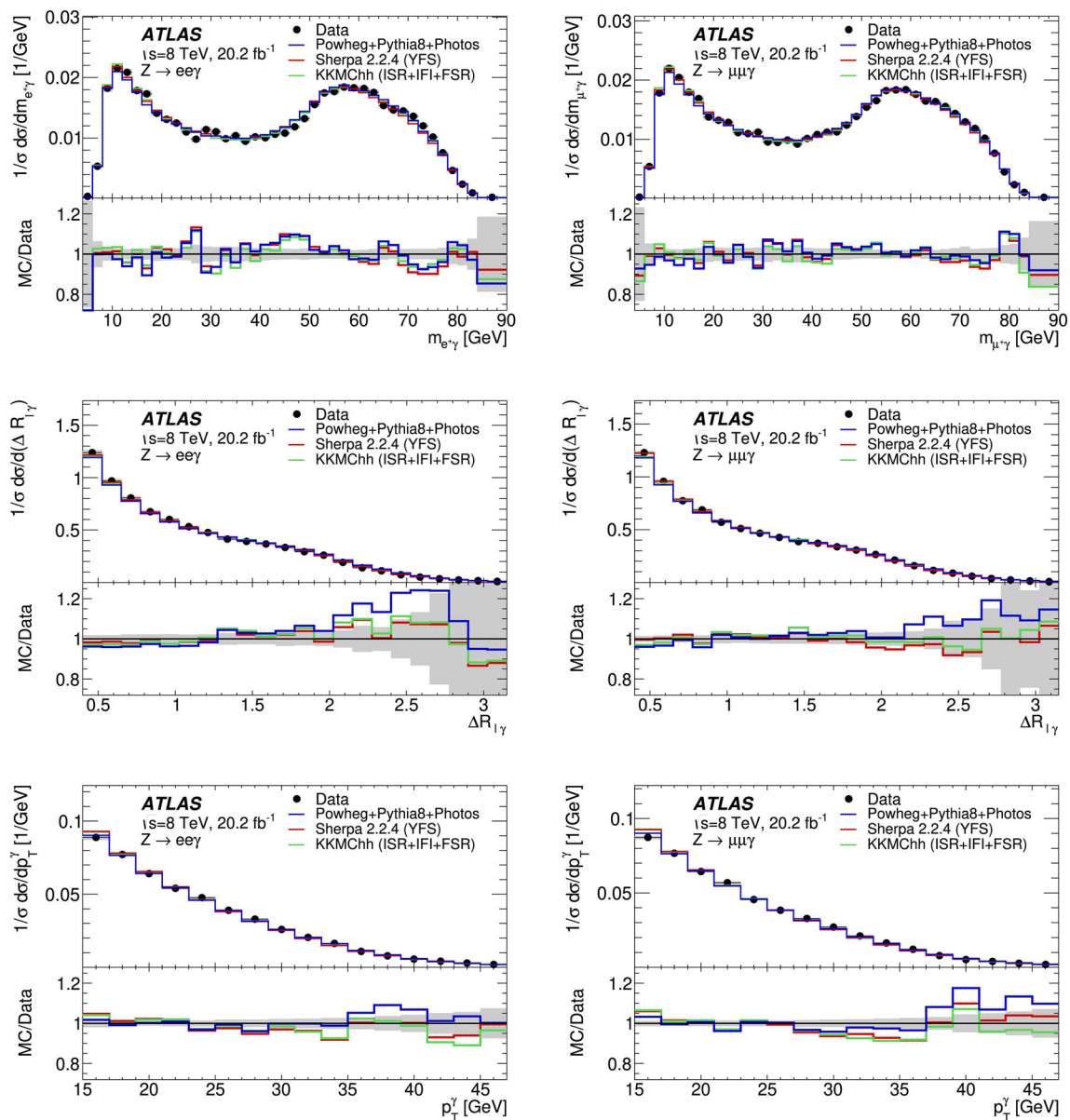


Fig. 7 Unfolded normalised differential fiducial cross-sections for the $Z \rightarrow ee\gamma$ (left) and $Z \rightarrow \mu\mu\gamma$ (right) channels. The results are shown in the case of bare leptons for the $m_{l+\gamma}$ (top), $\Delta R_{l\gamma}$ (middle), and p_T^γ (bottom) distributions. The data are compared to the predictions from Powheg+Pythia8+Photos, Sherpa 2.2.4, and KKMChh.

The bottom panels represent the ratios of these predictions to the data, where the gray band around unity represents the total data uncertainties and the dashed lines around the predictions represent their respective total uncertainties (see text).

Table 4 Uncertainties in the integrated fiducial cross-section measurements. The values for bare leptons with $m_{ll} > 20$ GeV are shown

Uncertainty	$Z \rightarrow ee\gamma$ (%)	$Z \rightarrow \mu\mu\gamma$ (%)
Statistical	0.7	0.7
Experimental systematic	3.5	2.3
Luminosity	1.9	1.9
QCD theory	0.3	0.3
Total	4.1	3.1

that the contributions from QED ISR and IFI are even smaller. The combined QED ISR/IFI contribution in the fiducial region of the analysis presented in this paper has been estimated with KKMChh to be 3×10^{-3} for the integrated fiducial cross-sections, with an uncertainty below 10^{-3} . These results have been confirmed using the CompHEP [37] code. In the case of the Sherpa 2.2.4 predictions which are also shown in Fig. 7, the uncertainty band is much larger and probably over-conservative, about 2%. This was estimated

Table 5 Integrated fiducial cross-sections (pb) for three ranges of the dilepton mass m_{ll} . The measurements are presented for bare leptons with the breakdown of their uncertainties together with the predictions from Powheg+Pythia8+Photos normalised as described in the text

Cross-sections in pb	Measurement	Prediction
$Z \rightarrow ee\gamma$ ($20 < m_{ll} < 80$ GeV)	3.03 ± 0.02 (stat) ± 0.11 (syst) ± 0.06 (lumi)	2.94 ± 0.10
$Z \rightarrow \mu\mu\gamma$ ($20 < m_{ll} < 80$ GeV)	3.17 ± 0.02 (stat) ± 0.07 (syst) ± 0.07 (lumi)	3.20 ± 0.10
$Z \rightarrow ee\gamma$ ($45 < m_{ll} < 80$ GeV)	2.70 ± 0.02 (stat) ± 0.10 (syst) ± 0.06 (lumi)	2.61 ± 0.10
$Z \rightarrow \mu\mu\gamma$ ($45 < m_{ll} < 80$ GeV)	2.84 ± 0.02 (stat) ± 0.06 (syst) ± 0.06 (lumi)	2.84 ± 0.10
$Z \rightarrow ee\gamma$ ($20 < m_{ll} < 45$ GeV)	0.326 ± 0.005 (stat) ± 0.011 (syst) ± 0.006 (lumi)	0.335 ± 0.01
$Z \rightarrow \mu\mu\gamma$ ($20 < m_{ll} < 45$ GeV)	0.321 ± 0.005 (stat) ± 0.006 (syst) ± 0.006 (lumi)	0.355 ± 0.01

using a recipe similar to that described in [38], corresponding to higher-order QED corrections which are only known at the Z -boson pole and are not applied outside a very narrow region around m_Z to assess this uncertainty.

The agreement between the measurements and the predictions from the MC simulations is reasonable for all three distributions over most of their range, both for electrons and muons. The agreement between the predictions themselves is better for $m_{l+\gamma}$ than their respective agreement with the data, suggesting perhaps that most of the fluctuations seen in the ratio plots for this observable are related to statistical fluctuations in the data since they are limited to a few bins. However, there is a noticeable discrepancy between the measurement in the electron channel and the Powheg+Pythia8+Photos prediction for values of $\Delta R_{l\gamma}$ larger than 2.5, at the edge of the phase space where the two leptons from Z -boson decay recoil against the photon.

8.2 Integrated fiducial cross-sections

The normalised differential fiducial cross-section measurements presented above are only sensitive to the shape of the distributions, but they benefit from cancellations of experimental systematic uncertainties for the sources that do not vary much with lepton p_T , such as the lepton efficiencies. This section presents the integrated fiducial cross-section measurements in the electron and muon channels and discusses the results for three different ranges of the dilepton mass. The uncertainties in the integrated fiducial cross-sections are summarised in Table 4. They include the uncertainty of 1.9% in the integrated luminosity and are somewhat larger for some of the experimental sources than are those listed in more detail in Table 3 for the reasons explained above.

The comparisons between the measured integrated cross-sections over three different dilepton mass ranges and the corresponding theory predictions, normalised to the QCD NNLO prediction used in [39] for the total inclusive cross-section for Z -boson production, are presented in Table 5. The agreement between the measurements and the predictions is reasonable within their comparable overall uncertain-

ties. The uncertainties in the theory predictions are also taken from [39]. As explained in Sect. 1 and shown in Table 5 for the theory predictions, the cross-sections for the $Z \rightarrow \mu\mu\gamma$ process are expected to be larger than those for the $Z \rightarrow ee\gamma$ process. This difference is enhanced significantly in this measurement by the higher acceptance, due to the pseudorapidity coverage, of the $Z \rightarrow \mu\mu\gamma$ channel with respect to the $Z \rightarrow ee\gamma$ channel.

9 First measurement of the $Z \rightarrow ll\gamma\gamma$ process

This section presents a first measurement of the $Z \rightarrow ll\gamma\gamma$ process at the LHC (Fig. 8). Given the limited statistics expected for the dataset considered here, the candidate event samples for each charged lepton flavour were combined together, and the selection requirements on the sub-leading photon were loosened with respect to the leading one. The sample considered was the same one as for the $Z \rightarrow ll\gamma$ analysis in terms of the charged lepton requirements, with however a tighter selection requirement of $p_T > 15$ GeV for the softer of the two leptons, but without any requirement on the dilepton mass. The two photons were required to be within the same pseudorapidity range as for the $Z \rightarrow ll\gamma$ analysis with thresholds in p_T set to respectively 15 and 10 GeV and within an angular distance, $\Delta R_{l\gamma}$ of at least 0.4 from each charged lepton. In addition, the angular distance between the two photons, $\Delta R_{\gamma\gamma}$, was also required to be larger than 0.4. Figure 9 (top left) shows the invariant mass of the two leptons and two photons, $m_{ll\gamma\gamma}$, versus the invariant mass of the two leptons and the highest p_T photon, $m_{ll\gamma}$. As illustrated in this figure, for values of $m_{ll\gamma}$ larger than 80 GeV, significant contributions of background from $Z \rightarrow ll\gamma$ +jet(s) events and from $Z \rightarrow ll$ +jets events are expected.

In order to reduce these contributions as well as possible contributions from $Z \rightarrow ll\gamma$ events with initial state QED radiation to the percent level or less, the invariant mass, $m_{ll\gamma}$, was required to be below 80 GeV for both photons. These requirements are summarised as fiducial volume selections in Table 6. A total of 116 events, corresponding to 61 electron pairs and 55 muon pairs, were thus selected as $Z \rightarrow ll\gamma\gamma$

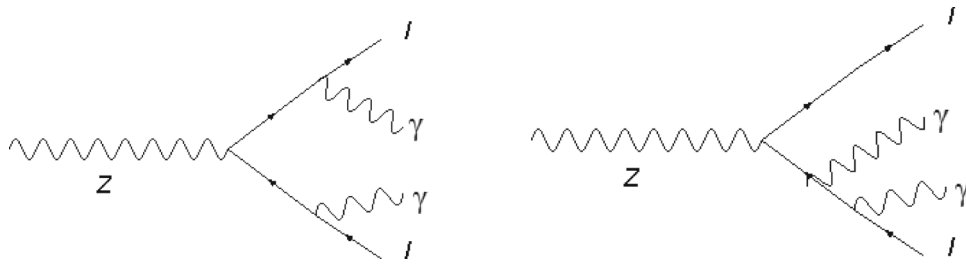


Fig. 8 Examples of $Z \rightarrow ll\gamma\gamma$ final-state radiation diagrams

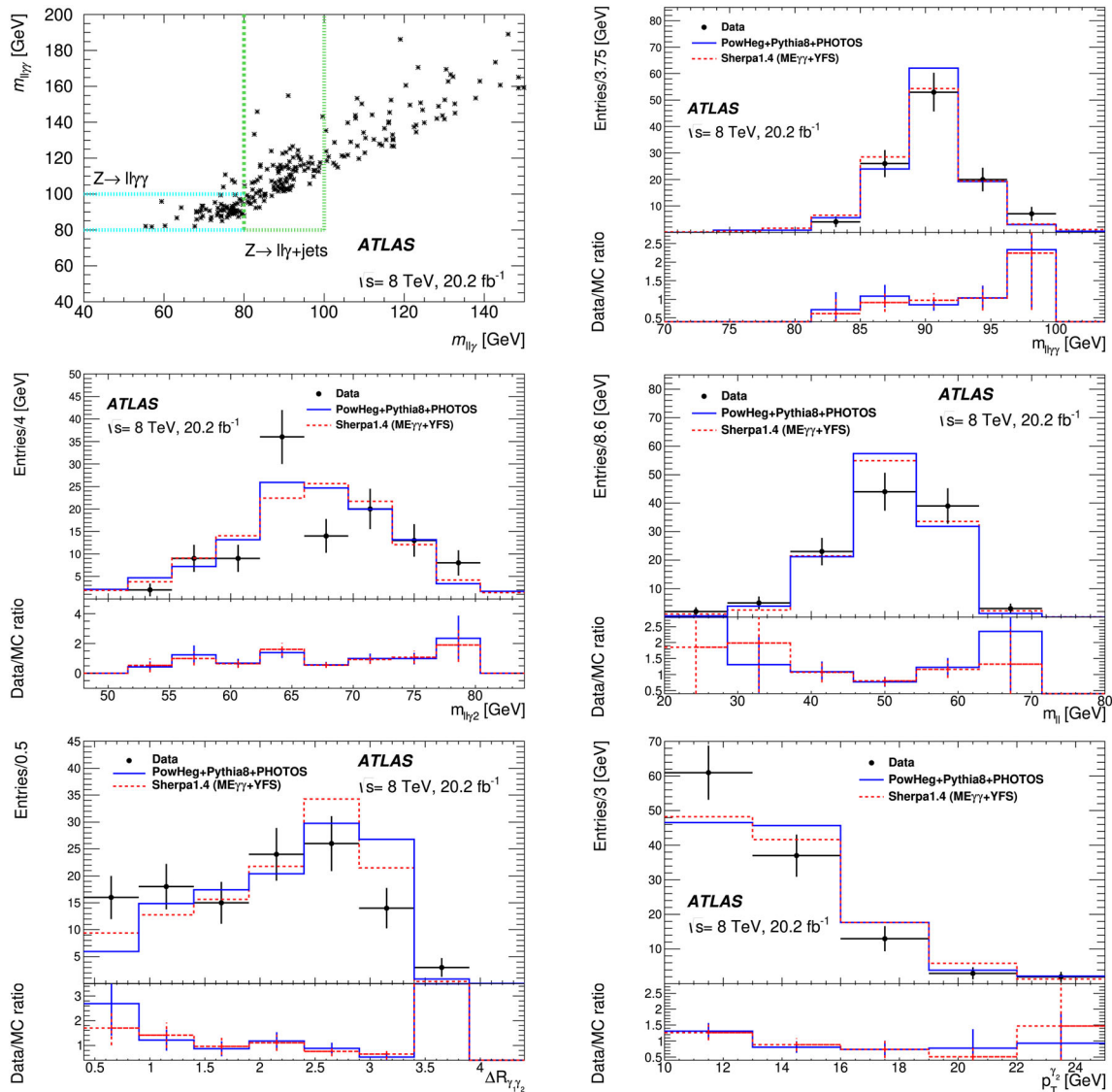


Fig. 9 For all selected $Z \rightarrow ll\gamma\gamma$ candidates before applying any selection on the invariant mass of the two leptons and each photon described in the text, distribution of invariant mass of the two leptons and of the two photons, $m_{ll\gamma\gamma}$ versus the invariant mass of the two leptons and of the highest p_T photon, $m_{ll\gamma}$ (top left). The horizontal dashed (blue) rectangle indicates the region where the $Z \rightarrow ll\gamma\gamma$ signal is expected and the vertical dashed (green) rectangle indicates the region dominated by background from $Z \rightarrow ll\gamma$ events accompanied by one

or more jets. Also shown after all selection requirements are the distributions of the total invariant mass (top right), of the invariant mass of the two leptons and the second photon, of the dilepton mass, of the angular distance between the two photons, and of the transverse momentum of the second photon. The data are compared to predictions from PowHeg+Pythia8+PhOTOS and Sherpa 1.4 ME $_{\gamma\gamma}$, normalised both to the data. The results are shown for bare leptons, and electrons and muons have been combined. The uncertainties shown are statistical

Table 6 Fiducial volume selections for $Z \rightarrow ll\gamma\gamma$ events

Two photons with $p_T > 15$ and 10 GeV, respectively
 $|\eta_\gamma| < 2.37$ excluding $1.37 < |\eta_\gamma| < 1.52$
 Two same-flavour opposite-sign leptons with $p_T > 25, 15$ GeV
 $|\eta_\mu| < 2.7$
 $|\eta_e| < 2.47$
 $\Delta R_{l\gamma} > 0.4$ for both photons, $\Delta R_{\gamma\gamma} > 0.4$
 $m_{ll\gamma} < 80$ GeV for both photons

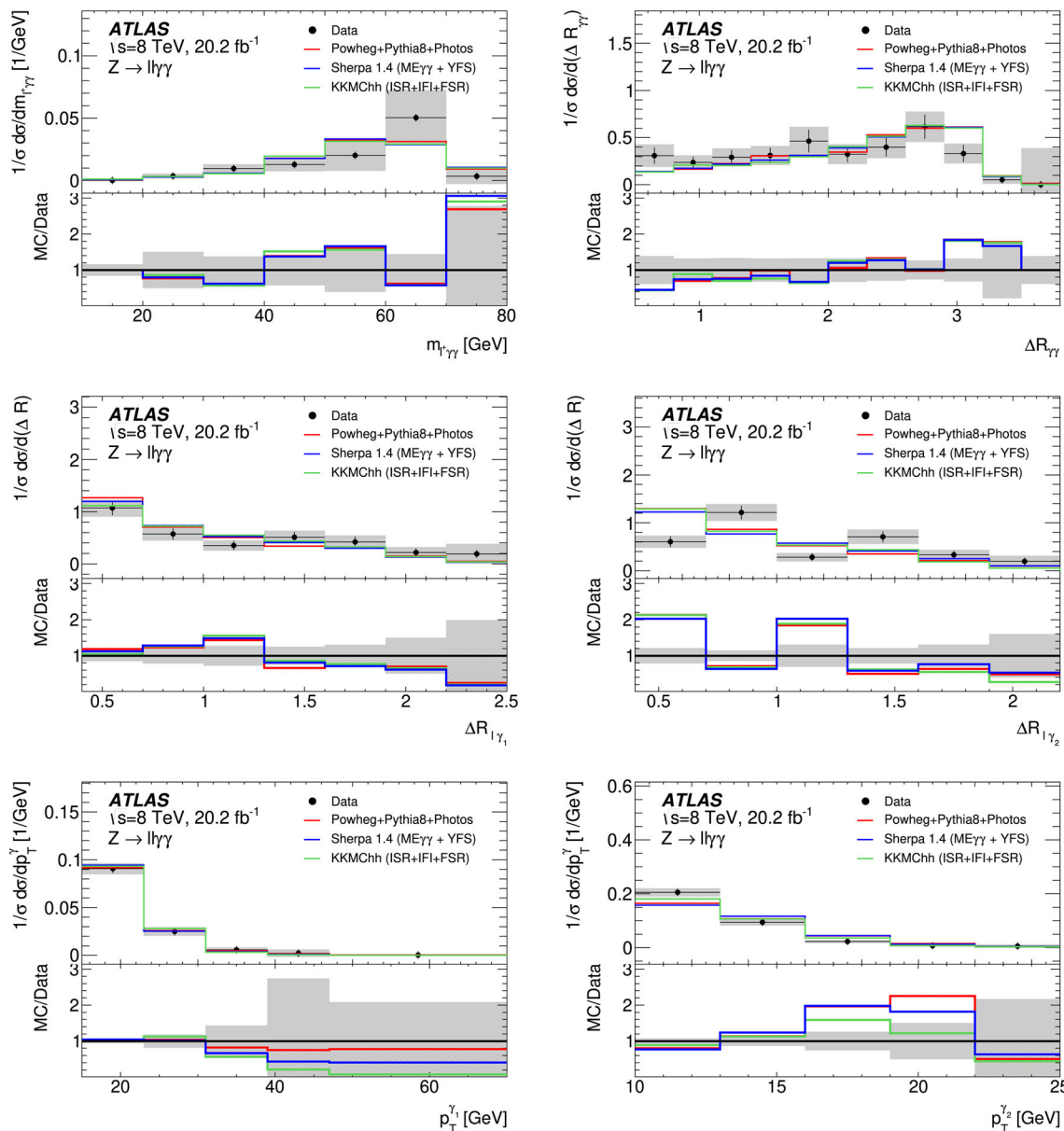


Fig. 10 For all selected $Z \rightarrow ll\gamma\gamma$ candidates, unfolded normalised distributions of $m_{l\gamma\gamma}$ (top left), of $\Delta R_{\gamma\gamma}$ (top right), of the angular distance between the first (middle left) and second (middle right) photon and the closest lepton, and of the transverse momentum spectrum of the two photons (bottom). The unfolded data are compared to predic-

tions from Powheg+Pythia8+Photos, Sherpa 1.4 $ME_{\gamma\gamma}$, and KKMChh. The results are shown for bare leptons, and electrons and muons have been combined. The gray band represents the total data uncertainties and the dashed lines around the predictions represent their statistical uncertainties, which are dominant, for the predictions

candidates. The dominant background from $Z \rightarrow ll\gamma$ +jet events was estimated by applying the same two-dimensional sideband method as that described for the main analysis: the quality and isolation criteria were inverted for the second photon. The background was found to be less than one event and Fig. 9 (top right) illustrates this through the observed distribution of $m_{ll\gamma\gamma}$ which displays no events outside the pole region.

The data were compared to MC $Z \rightarrow ll\gamma\gamma$ samples produced using the same Powheg+Pythia8+Photos version used for the main analysis, Sherpa 1.4 ME $_{\gamma\gamma}$ (see Sect. 3), and KKMChh. Figure 9 (top right, middle and bottom) shows that the predictions describe the data within their large statistical uncertainties for a selection of observables.

Finally, the data were corrected for detector efficiencies and resolution, and fiducial cross-sections were extracted together with unfolded distributions of several observables. The fiducial cross-section is measured to be 22.2 ± 2.1 (stat) ± 1.2 (exp) ± 4.1 (theo) fb for bare leptons. In contrast to the $Z \rightarrow ll\gamma$ case, the expected efficiencies from the Sherpa 1.4 ME $_{\gamma\gamma}$ and Powheg+Pythia8+Photos MC samples are significantly different and this difference was included as an additional theoretical systematic uncertainty in the measurement result for the $Z \rightarrow ll\gamma\gamma$ cross-section quoted here.

The expected fiducial cross-section from Sherpa 1.4 ME $_{\gamma\gamma}$ is 9.9 ± 0.1 (stat) fb, that from Powheg+Pythia8+Photos is 9.4 ± 0.3 (stat) fb. Both values are significantly smaller than the measured one. However, the expected fiducial cross-section from Sherpa 2.2.4 is 20.9 ± 0.2 (stat) fb, in agreement with the data. Although the purely QED systematic uncertainty in the predictions cannot explain the observed discrepancies between the measurement and two of the predictions, the overall systematic uncertainty in the predictions, which should include QCD and mixed QCD/QED effects, is not known. This uncertainty is clearly of QCD origin, as shown by the two versions of Sherpa. Figure 10 shows the unfolded distributions for the data compared to the predictions. The uncertainties shown are the combined statistical and systematic uncertainties for the data and only the statistical uncertainties for the predictions. The agreement in shape between data and predictions is reasonable within the uncertainties of this first measurement.

10 Conclusions

This paper presents the first ATLAS measurement of unfolded normalised differential fiducial cross-sections for $Z \rightarrow ee\gamma$ and $Z \rightarrow \mu\mu\gamma$ final states together with a few integrated fiducial cross-sections. The overall accuracy of the differential measurements is at the 1–2% level over a large fraction of the overall phase space, with an average overall systematic

uncertainty of 0.6% for the chosen observables, $m_{l+\gamma}$, $\Delta R_{l\gamma}$, and p_T^γ .

The results are in agreement with predictions of MC generators containing state-of-the-art QED FSR calculations such as Photos (in PowHeg+Pythia8+Photos) and YFS (in Sherpa 2.2.4). They are also in agreement with the recent calculations of KKMChh which provides a consistent and gauge-invariant breakdown of the different contributions to final states containing two charged leptons and a high- p_T photon, and thus demonstrates that the QED ISR and IFI contributions are very small for the fiducial selections of the analysis described in this paper.

Finally, the $Z \rightarrow ll\gamma\gamma$ process has been observed for the first time. The differential distributions for this process are described by the available calculations within present large statistical uncertainties of the measurement. The $Z \rightarrow ll\gamma\gamma$ fiducial cross-section is consistent with Sherpa 2.2.4 and is twice as large as predicted by PowHeg+Pythia8+Photos and Sherpa 1.4 ME $_{\gamma\gamma}$.

Acknowledgements We thank CERN for the very successful operation of the LHC, as well as the support staff from our institutions without whom ATLAS could not be operated efficiently. We acknowledge the support of ANPCyT, Argentina; YerPhi, Armenia; ARC, Australia; BMWFW and FWF, Austria; ANAS, Azerbaijan; CNPq and FAPESP, Brazil; NSERC, NRC and CFI, Canada; CERN; ANID, Chile; CAS, MOST and NSFC, China; Minciencias, Colombia; MEYS CR, Czech Republic; DNRF and DNSRC, Denmark; IN2P3-CNRS and CEA-DRF/IRFU, France; SRNSFG, Georgia; BMBF, HGF and MPG, Germany; GSRI, Greece; RGC and Hong Kong SAR, China; ISF and Benozzi Center, Israel; INFN, Italy; MEXT and JSPS, Japan; CNRST, Morocco; NWO, Netherlands; RCN, Norway; MEiN, Poland; FCT, Portugal; MNE/IFA, Romania; MOST, Serbia; MSSR, Slovakia; ARRS and MIZŠ, Slovenia; DSI/NRF, South Africa; MICINN, Spain; SRC and Wallenberg Foundation, Sweden; SERI, SNSF and Cantons of Bern and Geneva, Switzerland; MOST, Taiwan; TENMAK, Türkiye; STFC, United Kingdom; DOE and NSF, United States of America. In addition, individual groups and members have received support from BCKDF, CANARIE, Compute Canada and CRC, Canada; PRIMUS 21/SCI/017 and UNCE SCI/013, Czech Republic; COST, ERC, ERDF, Horizon 2020 and Marie Skłodowska-Curie Actions, European Union; Investissements d’Avenir Labex, Investissements d’Avenir IDEX and ANR, France; DFG and AvH Foundation, Germany; Herakleitos, Thales and Aristeia programmes co-financed by EU-ESF and the Greek NSRF, Greece; BSF-NSF and MINERVA, Israel; Norwegian Financial Mechanism 2014–2021, Norway; NCN and NAWA, Poland; La Caixa Banking Foundation, CERCA Programme Generalitat de Catalunya and PROMETEO and GenT Programmes Generalitat Valenciana, Spain; Göran Gustafssons Stiftelse, Sweden; The Royal Society and Leverhulme Trust, United Kingdom. The crucial computing support from all WLCG partners is acknowledged gratefully, in particular from CERN, the ATLAS Tier-1 facilities at TRIUMF (Canada), NDGF (Denmark, Norway, Sweden), CC-IN2P3 (France), KIT/GridKA (Germany), INFN-CNAF (Italy), NL-T1 (Netherlands), PIC (Spain), ASGC (Taiwan), RAL (UK) and BNL (USA), the Tier-2 facilities worldwide and large non-WLCG resource providers. Major contributors of computing resources are listed in Ref. [40].

Data availability This manuscript has no associated data or the data will not be deposited. [Authors’ comment: The data for this manuscript

are not available. The values in the plots and tables associated to this article are stored in HEPDATA (<https://hepdata.cedar.ac.uk/>.)

Open Access This article is licensed under a Creative Commons Attribution 4.0 International License, which permits use, sharing, adaptation, distribution and reproduction in any medium or format, as long as you give appropriate credit to the original author(s) and the source, provide a link to the Creative Commons licence, and indicate if changes were made. The images or other third party material in this article are included in the article's Creative Commons licence, unless indicated otherwise in a credit line to the material. If material is not included in the article's Creative Commons licence and your intended use is not permitted by statutory regulation or exceeds the permitted use, you will need to obtain permission directly from the copyright holder. To view a copy of this licence, visit <http://creativecommons.org/licenses/by/4.0/>.

Funded by SCOAP³.

References

- ATLAS Collaboration, Measurement of the W-boson mass in pp collisions at $\sqrt{s} = 7$ TeV with the ATLAS detector. *Eur. Phys. J. C* **78**, 110 (2018) [Erratum: *Eur. Phys. J. C* **78**, 898 (2018)]. [arXiv:1701.07240](https://arxiv.org/abs/1701.07240) [hep-ex]
- S. Jadach, B.F.L. Ward, Z.A. Was, S.A. Yost, Initial-final-interference and initial-state-radiation effects for Z/γ^* Drell–Yan observables using KKMC-hh (2020). [arXiv:2002.11692](https://arxiv.org/abs/2002.11692)
- D. Yennie, S. Frautschi, H. Suura, The infrared divergence phenomena and high-energy processes. *Ann. Phys.* **13**, 379 (1961)
- S. Jadach, B. Ward, Z. Was, Coherent exclusive exponentiation for precision Monte Carlo calculations. *Phys. Rev. D* **63**, 113009 (2001). [arXiv: hep-ph/0006359](https://arxiv.org/abs/hep-ph/0006359)
- S. Jadach, B.F.L. Ward, Z.A. Was, S.A. Yost, KK MC-hh: resummed exact $\mathcal{O}(\alpha^2 L)$ EW corrections in a hadronic MC event generator. *Phys. Rev. D* **94**, 074006 (2016). [arXiv: 1608.01260](https://arxiv.org/abs/1608.01260)
- S. Jadach, B.F.L. Ward, Z.A. Was, S.A. Yost, KK MC-hh: systematic studies of exact $\mathcal{O}(\alpha^2 L)$ CEXX EW corrections in a hadronic MC for precision Z/γ^* physics at LHC energies. *Phys. Rev. D* **99**, 076016 (2019) [We are very grateful to S. Yost for providing the calculations from KKMChh], [arXiv:1707.06502](https://arxiv.org/abs/1707.06502)
- T. Gleisberg et al., Event generation with SHERPA 1.1. *JHEP* **02**, 007 (2009). [arXiv:0811.4622](https://arxiv.org/abs/0811.4622) [hep-ph]
- E. Bothmann et al., Event generation with Sherpa 2.2. *SciPost Phys.* **7**, 034 (2019). [arXiv:1905.09127](https://arxiv.org/abs/1905.09127) [hep-ph]
- P. Golonka, Z. Was, Next to leading logarithms and the PHOTOS Monte Carlo. *Eur. Phys. J. C* **50**, 53 (2007). [arXiv:hep-ph/0604232](https://arxiv.org/abs/hep-ph/0604232)
- P. Nason, A new method for combining NLO QCD with shower Monte Carlo algorithms. *JHEP* **11**, 040 (2004). [arXiv:hep-ph/0409146](https://arxiv.org/abs/hep-ph/0409146)
- S. Frixione, P. Nason, C. Oleari, Matching NLO QCD computations with parton shower simulations: the POWHEG method. *JHEP* **11**, 070 (2007). [arXiv:0709.2092](https://arxiv.org/abs/0709.2092) [hep-ph]
- S. Alioli, P. Nason, C. Oleari, E. Re, A general framework for implementing NLO calculations in shower Monte Carlo programs: the POWHEG BOX. *JHEP* **06**, 043 (2010). [arXiv:1002.2581](https://arxiv.org/abs/1002.2581) [hep-ph]
- S. Alioli, P. Nason, C. Oleari, E. Re, NLO vector-boson production matched with shower in POWHEG. *JHEP* **07**, 060 (2008). [arXiv:0805.4802](https://arxiv.org/abs/0805.4802) [hep-ph]
- T. Sjostrand, S. Mrenna, P. Skands, A brief introduction to PYTHIA 8.1. *Comput. Phys. Commun.* **178**, 852 (2008). [arXiv:0710.3820](https://arxiv.org/abs/0710.3820) [hep-ph]
- M. Schoenherr, F. Krauss, Soft photon radiation in particle decays in SHERPA. *JHEP* **12**, 018 (2008). [arXiv:0810.5071](https://arxiv.org/abs/0810.5071)
- F. Krauss, J. Lindert, R. Linten, Accurate simulation of W, Z, and Higgs boson decays in SHERPA. *Eur. Phys. J. C* **79**, 143 (2019). [arXiv:1212.6783](https://arxiv.org/abs/1212.6783)
- ATLAS Collaboration, The ATLAS experiment at the CERN Large Hadron Collider, JINST **3**, S08003 (2008)
- ATLAS Collaboration, The ATLAS Collaboration Software and Firmware, ATL-SOFT-PUB-2021-001 (2021). <https://cds.cern.ch/record/2767187>
- J. Pumplin et al., New generation of parton distributions with uncertainties from global QCD analysis. *JHEP* **07**, 012 (2002). [arXiv:hep-ph/0201195](https://arxiv.org/abs/hep-ph/0201195)
- ATLAS Collaboration, Summary of ATLAS Pythia 8 tunes, ATL-PHYS-PUB-2012-003 (2012). <https://cds.cern.ch/record/1474107>
- N. Davidson, T. Przedzinski, Z. Was, PHOTOS Interface in C++: technical and physics documentation. *Comput. Phys. Commun.* **199**, 86 (2016). [arXiv:1011.0937](https://arxiv.org/abs/1011.0937) [hep-ph]
- H.-L. Lai et al., New parton distributions for collider physics. *Phys. Rev. D* **82**, 074024 (2010). [arXiv:1007.2241](https://arxiv.org/abs/1007.2241) [hep-ph]
- S. Hoeche, F. Krauss, M. Schonherr, F. Siegert, QCD matrix elements + parton showers: the NLO case. *JHEP* **04**, 027 (2013). [arXiv:1207.5030](https://arxiv.org/abs/1207.5030) [hep-ph]
- T. Sjöstrand, S. Mrenna, P.Z. Skands, PYTHIA 6.4 physics and manual. *JHEP* **05**, 026 (2006). [arXiv:hep-ph/0603175](https://arxiv.org/abs/hep-ph/0603175)
- ATLAS Collaboration, The ATLAS simulation infrastructure. *Eur. Phys. J. C* **70**, 823 (2010). [arXiv:1005.4568](https://arxiv.org/abs/1005.4568) [physics.ins-det]
- S. Agostinelli et al., Geant4—a simulation toolkit. *Nucl. Instrum. Meth. A* **506**, 250 (2003)
- ATLAS Collaboration, Electron and photon performance measurements with the ATLAS detector using the 2015–2017 LHC proton–proton collision data. *JINST* **14**, P12006 (2019). [arXiv:1908.00005](https://arxiv.org/abs/1908.00005) [hep-ex]
- ATLAS Collaboration, Measurement of the photon identification efficiencies with the ATLAS detector using LHC Run-1 data. *Eur. Phys. J. C* **76**, 666 (2016). [arXiv:1606.01813](https://arxiv.org/abs/1606.01813) [hep-ex]
- ATLAS Collaboration, Electron efficiency measurements with the ATLAS detector using 2012 LHC proton–proton collision data. *Eur. Phys. J. C* **77**, 195 (2017). [arXiv:1612.01456](https://arxiv.org/abs/1612.01456) [hep-ex]
- ATLAS Collaboration, Measurement of the muon reconstruction performance of the ATLAS detector using 2011 and 2012 LHC proton–proton collision data. *Eur. Phys. J. C* **74**, 3130 (2014). [arXiv:1407.3935](https://arxiv.org/abs/1407.3935) [hep-ex]
- ATLAS Collaboration, Topological cell clustering in the ATLAS calorimeters and its performance in LHC Run 1. *Eur. Phys. J. C* **77**, 490 (2017). [arXiv:1603.02934](https://arxiv.org/abs/1603.02934) [hep-ex]
- M. Cacciari, G.P. Salam, G. Soyez, The catchment area of jets. *JHEP* **04**, 005 (2008). [arXiv:0802.1188](https://arxiv.org/abs/0802.1188) [hep-ph]
- M. Cacciari, G.P. Salam, S. Sapeta, On the characterisation of the underlying event. *JHEP* **04**, 065 (2010). [arXiv:0912.4926](https://arxiv.org/abs/0912.4926) [hep-ph]
- ATLAS Collaboration, Measurement of the inclusive isolated prompt photon cross section in pp collisions at $\sqrt{s} = 7$ TeV with the ATLAS detector. *Phys. Rev. D* **83**, 052005 (2011). [arXiv:1012.4389](https://arxiv.org/abs/1012.4389) [hep-ex]
- T. Auyeub, Unfolding algorithms and tests using RooUnfold, 313 (2011). [arXiv:1105.1160](https://arxiv.org/abs/1105.1160)
- ATLAS Collaboration, Measurement of the angular coefficients in Z-boson events using electron and muon pairs from data taken at $\sqrt{s} = 8$ TeV with the ATLAS detector. *JHEP* **08**, 159 (2016). [arXiv:1606.00689](https://arxiv.org/abs/1606.00689) [hep-ex]
- E. Boos et al., CompHEP 4.4. automatic computations from Lagrangians to events. *Nucl. Instrum. Meth. A* **534**, 250 (2004). Proceedings of the IXth International Workshop on Advanced Computing and Analysis Techniques in Physics Research, ISSN:0168-9002. [arXiv:hep-ph/0403113](https://arxiv.org/abs/hep-ph/0403113)

38. C. Gutsche, M. Schonherr, Four lepton production and the accuracy of QED FSR. *Eur. Phys. J. C* **81**, 48 (2021). [arXiv:2007.15360](https://arxiv.org/abs/2007.15360) [hep-ph]
39. ATLAS Collaboration, Measurements of top-quark pair to Z-boson cross-section ratios at $\sqrt{s} = 13, 8, 7$ TeV with the ATLAS detector. *JHEP* **02**, 117 (2017). [arXiv:1612.03636](https://arxiv.org/abs/1612.03636) [hep-ex]
40. ATLAS Collaboration, ATLAS Computing Acknowledgements, ATL-SOFT-PUB-2023-001 (2023). <https://cds.cern.ch/record/2869272>

ATLAS Collaboration*

G. Aad¹⁰¹, B. Abbott¹¹⁹, D. C. Abbott¹⁰², K. Abeling⁵⁵, S. H. Abidi²⁹, A. Abouhorma^{35e}, H. Abramowicz¹⁵⁰, H. Abreu¹⁴⁹, Y. Abulaiti¹¹⁶, A. C. Abusleme Hoffman^{136a}, B. S. Acharya^{68a,68b,q}, B. Achkar⁵⁵, C. Adam Bourdarios⁴, L. Adamczyk^{84a}, L. Adamek¹⁵⁴, S. V. Addepalli²⁶, J. Adelman¹¹⁴, A. Adiguzel^{21c}, S. Adorni⁵⁶, T. Auyeub¹³³, A. A. Affolder¹³⁵, Y. Afik³⁶, M. N. Agaras¹³, J. Agarwala^{72a,72b}, A. Aggarwal⁹⁹, C. Agheorghiesei^{27c}, J. A. Aguilar-Saavedra^{129f}, A. Ahmad³⁶, F. Ahmadov^{38,ab}, W. S. Ahmed¹⁰³, S. Ahuja⁹⁴, X. Ai⁴⁸, G. Aielli^{75a,75b}, I. Aizenberg¹⁶⁸, M. Akbiyik⁹⁹, T. P. A. Åkesson⁹⁷, A. V. Akimov³⁷, K. Al Khoury⁴¹, G. L. Alberghi^{23b}, J. Albert¹⁶⁴, P. Albicocco⁵³, S. Alderweireldt⁵², M. Aleksa³⁶, I. N. Aleksandrov³⁸, C. Alexa^{27b}, T. Alexopoulos¹⁰, A. Alfonsi¹¹³, F. Alfonsi^{23b}, M. Alhroob¹¹⁹, B. Ali¹³¹, S. Ali¹⁴⁷, M. Aliev³⁷, G. Alimonti^{70a}, W. Alkhalaf⁵⁵, C. Allaire⁶⁶, B. M. M. Allbrooke¹⁴⁵, P. P. Allport²⁰, A. Aloisio^{71a,71b}, F. Alonso⁸⁹, C. Alpigiani¹³⁷, E. Alunno Camelia^{75a,75b}, M. Alvarez Estevez⁹⁸, M. G. Alvigi^{71a,71b}, M. Aly¹⁰⁰, Y. Amaral Coutinho^{81b}, A. Ambler¹⁰³, C. Amelung³⁶, M. Ameri¹, C. G. Ames¹⁰⁸, D. Amidei¹⁰⁵, S. P. Amor Dos Santos^{129a}, S. Amoroso⁴⁸, K. R. Amos¹⁶², V. Ananiev¹²⁴, C. Anastopoulos¹³⁸, T. Andeen¹¹, J. K. Anders³⁶, S. Y. Andreev^{47a,47b}, A. Andreazza^{70a,70b}, S. Angelidakis⁹, A. Angerami^{41,ae}, A. V. Anisenkov³⁷, A. Annovi^{73a}, C. Antel⁵⁶, M. T. Anthony¹³⁸, E. Antipov¹²⁰, M. Antonelli⁵³, D. J. A. Antrim^{17a}, F. Anulli^{74a}, M. Aoki⁸², T. Aoki¹⁵², J. A. Aparisi Pozo¹⁶², M. A. Aparo¹⁴⁵, L. Aperio Bella⁴⁸, C. Appelt¹⁸, N. Aranzabal³⁶, V. Araujo Ferraz^{81a}, C. Arcangeletti⁵³, A. T. H. Arce⁵¹, E. Arena⁹¹, J.-F. Arguin¹⁰⁷, S. Argyropoulos⁵⁴, J. H. Arling⁴⁸, A. J. Armbruster³⁶, O. Arnaez¹⁵⁴, H. Arnold¹¹³, Z. P. Arrubarrena Tame¹⁰⁸, G. Artoni^{74a,74b}, H. Asada¹¹⁰, K. Asai¹¹⁷, S. Asai¹⁵², N. A. Asbah⁶¹, K. Assamagan²⁹, R. Astalos^{28a}, R. J. Atkin^{33a}, M. Atkinson¹⁶¹, N. B. Atlay¹⁸, H. Atmani^{62b}, P. A. Atlasiddha¹⁰⁵, K. Augsten¹³¹, S. Auricchio^{71a,71b}, A. D. Aurilio²⁰, V. A. Austrup¹⁷⁰, G. Avner¹⁴⁹, G. Avolio³⁶, K. Axiotis⁵⁶, M. K. Ayoub^{14c}, G. Azuelos^{107,aj}, D. Babal^{28a}, H. Bachacou¹³⁴, K. Bachas^{151,t}, A. Bachi³⁴, F. Backman^{47a,47b}, A. Badea⁶¹, P. Bagnaia^{74a,74b}, M. Bahmani¹⁸, A. J. Bailey¹⁶², V. R. Bailey¹⁶¹, J. T. Baines¹³³, C. Bakalis¹⁰, O. K. Baker¹⁷¹, P. J. Bakker¹¹³, E. Bakos¹⁵, D. Bakshi Gupta⁸, S. Balaji¹⁴⁶, R. Balasubramanian¹¹³, E. M. Baldin³⁷, P. Balek¹³², E. Ballabene^{70a,70b}, F. Balli¹³⁴, L. M. Baltes^{63a}, W. K. Balunas³², J. Balz⁹⁹, E. Banas⁸⁵, M. Bandieramonte¹²⁸, A. Bandyopadhyay²⁴, S. Bansal²⁴, L. Barak¹⁵⁰, E. L. Barberio¹⁰⁴, D. Barberis^{57a,57b}, M. Barbero¹⁰¹, G. Barbour⁹⁵, K. N. Barends^{33a}, T. Barillari¹⁰⁹, M.-S. Barisits³⁶, T. Barklow¹⁴², R. M. Barnett^{17a}, P. Baron¹²¹, D. A. Baron Moreno¹⁰⁰, A. Baroncelli^{62a}, G. Barone²⁹, A. J. Barr¹²⁵, L. Barranco Navarro^{47a,47b}, F. Barreiro⁹⁸, J. Barreiro Guimarães da Costa^{14a}, U. Barron¹⁵⁰, M. G. Barros Teixeira^{129a}, S. Barsov³⁷, F. Bartels^{63a}, R. Bartoldus¹⁴², A. E. Barton⁹⁰, P. Bartos^{28a}, A. Basalae⁴⁸, A. Basan⁹⁹, M. Baselga⁴⁹, I. Bashta^{76a,76b}, A. Bassalat^{66,b}, M. J. Basso¹⁵⁴, C. R. Basson¹⁰⁰, R. L. Bates⁵⁹, S. Batlamous^{35e}, J. R. Batley³², B. Batool¹⁴⁰, M. Battaglia¹³⁵, D. Battulga¹⁸, M. Bauce^{74a,74b}, P. Bauer²⁴, A. Bayirli^{21a}, J. B. Beacham⁵¹, T. Beau¹²⁶, P. H. Beauchemin¹⁵⁷, F. Becherer⁵⁴, P. Bechtel²⁴, H. P. Beck^{19,s}, K. Becker¹⁶⁶, A. J. Beddall^{21d}, V. A. Bednyakov³⁸, C. P. Bee¹⁴⁴, L. J. Beemster¹⁵, T. A. Beermann³⁶, M. Begalli^{81d}, M. Begel²⁹, A. Behera¹⁴⁴, J. K. Behr⁴⁸, C. Beirao Da Cruz E Silva³⁶, J. F. Beirer^{36,55}, F. Beisiegel²⁴, M. Belfkir¹⁵⁸, G. Bella¹⁵⁰, L. Bellagamba^{23b}, A. Bellerive³⁴, P. Bellos²⁰, K. Beloborodov³⁷, K. Belotskiy³⁷, N. L. Belyaev³⁷, D. Benčekroun^{35a}, F. Bendebba^{35a}, Y. Benhammou¹⁵⁰, D. P. Benjamin²⁹, M. Benoit²⁹, J. R. Bensinger²⁶, S. Bentvelsen¹¹³, L. Beresford³⁶, M. Beretta⁵³, D. Berge¹⁸, E. Bergeas Kuutmann¹⁶⁰, N. Berger⁴, B. Bergmann¹³¹, J. Beringer^{17a}, S. Berlendis⁷, G. Bernardi⁵, C. Bernius¹⁴², F. U. Bernlochner²⁴, T. Berry⁹⁴, P. Berta¹³², A. Berthold⁵⁰, I. A. Bertram⁹⁰, S. Bethke¹⁰⁹, A. Betti^{74a,74b}, A. J. Bevan⁹³, M. Bhamjee^{33c}, S. Bhatta¹⁴⁴, D. S. Bhattacharya¹⁶⁵, P. Bhattarai²⁶, V. S. Bhopatkar¹²⁰, R. Bi^{29,am}, R. M. Bianchi¹²⁸, O. Biebel¹⁰⁸, R. Bielski¹²², M. Biglietti^{76a}, T. R. V. Billoud¹³¹, M. Bindi⁵⁵, A. Bingul^{21b}, C. Bini^{74a,74b}, S. Biondi^{23a,23b}, A. Biondini⁹¹, C. J. Birch-sykes¹⁰⁰, G. A. Bird^{20,133}, M. Birman¹⁶⁸, T. Bisanz³⁶, E. Bisceglie^{43a,43b}

D. Biswas^{169,m}, A. Bitadze¹⁰⁰, K. Bjørke¹²⁴, I. Bloch⁴⁸, C. Blocker²⁶, A. Blue⁵⁹, U. Blumenschein⁹³, J. Blumenthal⁹⁹, G. J. Bobbink¹¹³, V. S. Bobrovnikov³⁷, M. Boehler⁵⁴, D. Bogovac³⁶, A. G. Bogdanchikov³⁷, C. Bohm^{47a}, V. Boisvert⁹⁴, P. Bokan⁴⁸, T. Bold^{84a}, M. Bomben⁵, M. Bona⁹³, M. Boonekamp¹³⁴, C. D. Booth⁹⁴, A. G. Borbély⁵⁹, H. M. Borecka-Bielska¹⁰⁷, L. S. Borgna⁹⁵, G. Borissov⁹⁰, D. Bortoletto¹²⁵, D. Boscherini^{23b}, M. Bosman¹³, J. D. Bossio Sola³⁶, K. Bouaouda^{35a}, N. Bouchhar¹⁶², J. Boudreau¹²⁸, E. V. Bouhova-Thacker⁹⁰, D. Boumediene⁴⁰, R. Bouquet⁵, A. Boveia¹¹⁸, J. Boyd³⁶, D. Boye²⁹, I. R. Boyko³⁸, J. Bracinik²⁰, N. Brahimi^{62d}, G. Brandt¹⁷⁰, O. Brandt³², F. Braren⁴⁸, B. Brau¹⁰², J. E. Brau¹²², K. Brendlinger⁴⁸, R. Brenner¹⁶⁸, L. Brenner¹¹³, R. Brenner¹⁶⁰, S. Bressler¹⁶⁸, B. Brickwedde⁹⁹, D. Britton⁵⁹, D. Britzger¹⁰⁹, I. Brock²⁴, G. Brooijmans⁴¹, W. K. Brooks^{136f}, E. Brost²⁹, T. L. Bruckler¹²⁵, P. A. Bruckman de Renstrom⁸⁵, B. Brüers⁴⁸, D. Bruncko^{28b,*}, A. Bruni^{23b}, G. Bruni^{23b}, M. Bruschi^{23b}, N. Bruscinò^{74a,74b}, L. Bryngemark¹⁴², T. Buanes¹⁶, Q. Buat¹³⁷, P. Buchholz¹⁴⁰, A. G. Buckley⁵⁹, I. A. Budagov^{38,*}, M. K. Bugge¹²⁴, O. Bulekov³⁷, B. A. Bullard⁶¹, S. Burdin⁹¹, C. D. Burgard⁴⁸, A. M. Burger⁴⁰, B. Burghgrave⁸, J. T. P. Burr³², C. D. Burton¹¹, J. C. Burzynski¹⁴¹, E. L. Busch⁴¹, V. Büscher⁹⁹, P. J. Bussey⁵⁹, J. M. Butler²⁵, C. M. Buttar⁵⁹, J. M. Butterworth⁹⁵, W. Buttinger¹³³, C. J. Buxo Vazquez¹⁰⁶, A. R. Buzykaev³⁷, G. Cabras^{23b}, S. Cabrera Urbán¹⁶², D. Caforio⁵⁸, H. Cai¹²⁸, Y. Cai^{14a,14d}, V. M. M. Cairo³⁶, O. Cakir^{3a}, N. Calace³⁶, P. Calafiura^{17a}, G. Calderini¹²⁶, P. Calfayan⁶⁷, G. Callea⁵⁹, L. P. Caloba^{81b}, D. Calvet⁴⁰, S. Calvet⁴⁰, T. P. Calvet¹⁰¹, M. Calvetti^{73a,73b}, R. Camacho Toro¹²⁶, S. Camarda³⁶, D. Camarero Munoz²⁶, P. Camarri^{75a,75b}, M. T. Camerlingo^{76a,76b}, D. Cameron¹²⁴, C. Camincher¹⁶⁴, M. Campanelli⁹⁵, A. Camplani⁴², V. Canale^{71a,71b}, A. Canesse¹⁰³, M. Cano Bret⁷⁹, J. Cantero¹⁶², Y. Cao¹⁶¹, F. Capocasa²⁶, M. Capua^{43a,43b}, A. Carbone^{70a,70b}, R. Cardarelli^{75a}, J. C. J. Cardenas⁸, F. Cardillo¹⁶², T. Carli³⁶, G. Carlino^{71a}, J. I. Carlotto¹³, B. T. Carlson^{128,u}, E. M. Carlson^{155a,164}, L. Carminati^{70a,70b}, M. Carnesale^{74a,74b}, S. Caron¹¹², E. Carquin^{136f}, S. Carra^{70a}, G. Carratta^{23a,23b}, F. Carrio Argos^{33g}, J. W. S. Carter¹⁵⁴, T. M. Carter⁵², M. P. Casado^{13j}, A. F. Casha¹⁵⁴, E. G. Castiglia¹⁷¹, F. L. Castillo^{63a}, L. Castillo Garcia¹³, V. Castillo Gimenez¹⁶², N. F. Castro^{129a,129e}, A. Catinaccio³⁶, J. R. Catmore¹²⁴, V. Cavaliere²⁹, N. Cavalli^{23a,23b}, V. Cavasinni^{73a,73b}, E. Celebi^{21a}, F. Celli¹²⁵, M. S. Centonze^{69a,69b}, K. Cerny¹²¹, A. S. Cerqueira^{81a}, A. Cerri¹⁴⁵, L. Cerrito^{75a,75b}, F. Cerutti^{17a}, A. Cervelli^{23b}, S. A. Cetin^{21d}, Z. Chadi^{35a}, D. Chakraborty¹¹⁴, M. Chala^{129f}, J. Chan¹⁶⁹, W. Y. Chan¹⁵², J. D. Chapman³², B. Chargeishvili^{148b}, D. G. Charlton²⁰, T. P. Charman⁹³, M. Chatterjee¹⁹, S. Chekanov⁶, S. V. Chekulaev^{155a}, G. A. Chelkov^{38a}, A. Chen¹⁰⁵, B. Chen¹⁵⁰, B. Chen¹⁶⁴, H. Chen^{14c}, H. Chen²⁹, J. Chen^{62c}, J. Chen²⁶, S. Chen¹⁵², S. J. Chen^{14c}, X. Chen^{62c}, X. Chen^{14b,ai}, Y. Chen^{62a}, C. L. Cheng¹⁶⁹, H. C. Cheng^{64a}, S. Cheong¹⁴², A. Cheplakov³⁸, E. Cheremushkina⁴⁸, E. Cherepanova¹¹³, R. Cherkaoui El Moursli^{35c}, E. Cheu⁷, K. Cheung⁶⁵, L. Chevalier¹³⁴, V. Chiarella⁵³, G. Chiarelli^{73a}, N. Chiedde¹⁰¹, G. Chiodini^{69a}, A. S. Chisholm²⁰, A. Chitan^{27b}, M. Chitishvili¹⁶², Y. H. Chiu¹⁶⁴, M. V. Chizhov³⁸, K. Choi¹¹, A. R. Chomont^{74a,74b}, Y. Chou¹⁰², E. Y. S. Chow¹¹³, T. Chowdhury^{33g}, L. D. Christopher^{33g}, K. L. Chu^{64a}, M. C. Chu^{64a}, X. Chu^{14a,14d}, J. Chudoba¹³⁰, J. J. Chwastowski⁸⁵, D. Cieri¹⁰⁹, K. M. Ciesla^{84a}, V. Cindro⁹², A. Ciocio^{17a}, F. Ciotto^{71a,71b}, Z. H. Citron^{168,n}, M. Citterio^{70a}, D. A. Ciubotaru^{27b}, B. M. Ciungu¹⁵⁴, A. Clark⁵⁶, P. J. Clark⁵², J. M. Clavijo Columbie⁴⁸, S. E. Clawson¹⁰⁰, C. Clement^{47a,47b}, J. Clercx⁴⁸, L. Clissa^{23a,23b}, Y. Coadou¹⁰¹, M. Cobl^{68a,68c}, A. Coccaro^{57b}, R. F. Coelho Barrue^{129a}, R. Coelho Lopes De Sa¹⁰², S. Coelli^{70a}, H. Cohen¹⁵⁰, A. E. C. Coimbra^{70a,70b}, B. Cole⁴¹, J. Collot⁶⁰, P. Conde Muiño^{129a,129g}, M. P. Connell^{33c}, S. H. Connell^{33c}, I. A. Connelly⁵⁹, E. I. Conroy¹²⁵, F. Conventi^{71a,ak}, H. G. Cooke²⁰, A. M. Cooper-Sarkar¹²⁵, F. Cormier¹⁶³, L. D. Corpe³⁶, M. Corradi^{74a,74b}, E. E. Corrigan⁹⁷, F. Corriveau^{103,z}, A. Cortes-Gonzalez¹⁸, M. J. Costa¹⁶², F. Costanza⁴, D. Costanzo¹³⁸, B. M. Cote¹¹⁸, G. Cowan⁹⁴, J. W. Cowley³², K. Cranmer¹¹⁶, S. Crépe-Renaudin⁶⁰, F. Crescioli¹²⁶, M. Cristinziani¹⁴⁰, M. Cristoforetti^{77a,77b,d}, V. Croft¹⁵⁷, G. Crosetti^{43a,43b}, A. Cueto³⁶, T. Cuhadar Donszelmann¹⁵⁹, H. Cui^{14a,14d}, Z. Cui⁷, A. R. Cukierman¹⁴², W. R. Cunningham⁵⁹, F. Curcio^{43a,43b}, P. Czodrowski³⁶, M. M. Czurylo^{63b}, M. J. Da Cunha Sargedas De Sousa^{62a}, J. V. Da Fonseca Pinto^{81b}, C. Da Via¹⁰⁰, W. Dabrowski^{84a}, T. Dado⁴⁹, S. Dahbi^{33g}, T. Dai¹⁰⁵, C. Dallapiccola¹⁰², M. Dam⁴², G. D'amen²⁹, V. D'Amico¹⁰⁸, J. Damp⁹⁹, J. R. Dandoy¹²⁷, M. F. Daneri³⁰, M. Danninger¹⁴¹, V. Dao³⁶, G. Darbo^{57b}, S. Darmora⁶, S. J. Das^{29,am}, S. D'Auria^{70a,70b}, C. David^{155b}, T. Davidek¹³², D. R. Davis⁵¹, B. Davis-Purcell³⁴, I. Dawson⁹³, K. De⁸, R. De Asmundis^{71a}, M. De Beurs¹¹³, N. De Biase⁴⁸, S. De Castro^{23a,23b}, N. De Groot¹¹², P. de Jong¹¹³, H. De la Torre¹⁰⁶, A. De Maria^{14c}, A. De Salvo^{74a}, U. De Sanctis^{75a,75b}, A. De Santo¹⁴⁵, J. B. De Vivie De Regie⁶⁰, D. V. Dedovich³⁸, J. Degens¹¹³, A. M. Deiana⁴⁴, F. Del Corso^{23a,23b}, J. Del Peso⁹⁸, F. Del Rio^{63a}

F. Deliot¹³⁴, C. M. Delitzsch⁴⁹, M. Della Pietra^{71a,71b}, D. Della Volpe⁵⁶, A. Dell'Acqua³⁶, L. Dell'Asta^{70a,70b}, M. Delmastro⁴, P. A. Delsart⁶⁰, S. Demers¹⁷¹, M. Demichev³⁸, S. P. Denisov³⁷, L. D'Eramo¹¹⁴, D. Derendarz⁸⁵, F. Derue¹²⁶, P. Dervan⁹¹, K. Desch²⁴, K. Dette¹⁵⁴, C. Deutsch²⁴, P. O. Deviveiros³⁶, F. A. Di Bello^{57a,57b}, A. Di Ciaccio^{75a,75b}, L. Di Ciaccio⁴, A. Di Domenico^{74a,74b}, C. Di Donato^{71a,71b}, A. Di Girolamo³⁶, G. Di Gregorio⁵, A. Di Luca^{77a,77b}, B. Di Micco^{76a,76b}, R. Di Nardo^{76a,76b}, C. Diaconu¹⁰¹, F. A. Dias¹¹³, T. Dias Do Vale¹⁴¹, M. A. Diaz^{136a,136b}, F. G. Diaz Capriles²⁴, M. Didenko¹⁶², E. B. Diehl¹⁰⁵, L. Diehl⁵⁴, S. Díez Cornell⁴⁸, C. Diez Pardos¹⁴⁰, C. Dimitriadi^{24,160}, A. Dimitrievska^{17a}, W. Ding^{14b}, J. Dingfelder²⁴, I.-M. Dinu^{27b}, S. J. Dittmeier^{63b}, F. Dittus³⁶, F. Djama¹⁰¹, T. Djobava^{148b}, J. I. Djuvsland¹⁶, C. Doglioni^{97,100}, J. Dolejsi¹³², Z. Dolezal¹³², M. Donadelli^{81c}, B. Dong^{62c}, J. Donini⁴⁰, A. D'Onofrio^{14c}, M. D'Onofrio⁹¹, J. Dopke¹³³, A. Doria^{71a}, M. T. Dova⁸⁹, A. T. Doyle⁵⁹, M. A. Draguet¹²⁵, E. Drechsler¹⁴¹, E. Dreyer¹⁶⁸, I. Drivas-koulouris¹⁰, A. S. Drobac¹⁵⁷, M. Drozdova⁵⁶, D. Du^{62a}, T. A. du Pree¹¹³, F. Dubinin³⁷, M. Dubovsky^{28a}, E. Duchovni¹⁶⁸, G. Duckeck¹⁰⁸, O. A. Ducu^{27b}, D. Duda¹⁰⁹, A. Dudarev³⁶, M. D'uffizi¹⁰⁰, L. Duflot⁶⁶, M. Dührssen³⁶, C. Dülsen¹⁷⁰, A. E. Dumitriu^{27b}, M. Dunford^{63a}, S. Dungs⁴⁹, K. Dunne^{47a,47b}, A. Duperrin¹⁰¹, H. Duran Yildiz^{3a}, M. Düren⁵⁸, A. Durglishvili^{148b}, B. L. Dwyer¹¹⁴, G. I. Dyckes^{17a}, M. Dyndal^{84a}, S. Dysch¹⁰⁰, B. S. Dziejczak⁸⁵, Z. O. Earnshaw¹⁴⁵, B. Eckerova^{28a}, M. G. Eggleston⁵¹, E. Egidio Purcino De Souza^{81b}, L. F. Ehrke⁵⁶, G. Eigen¹⁶, K. Einsweiler^{17a}, T. Ekelof¹⁶⁰, P. A. Ekman⁹⁷, Y. El Ghazali^{35b}, H. El Jarrari^{35c,147}, A. El Moussaouy^{35a}, V. Ellajosyula¹⁶⁰, M. Ellert¹⁶⁰, F. Ellinghaus¹⁷⁰, A. A. Elliot⁹³, N. Ellis³⁶, J. Elmsheuser²⁹, M. Elsing³⁶, D. Emelianov¹³³, A. Emerman⁴¹, Y. Enari¹⁵², I. Ene^{17a}, S. Epari¹³, J. Erdmann^{49,ag}, A. Ereditato¹⁹, P. A. Erland⁸⁵, M. Errenst¹⁷⁰, M. Escalier⁶⁶, C. Escobar¹⁶², E. Etzion¹⁵⁰, G. Evans^{129a}, H. Evans⁶⁷, M. O. Evans¹⁴⁵, A. Ezhilov³⁷, S. Ezzarqtouni^{35a}, F. Fabbri⁵⁹, L. Fabbri^{23a,23b}, G. Facini⁹⁵, V. Fadeyev¹³⁵, R. M. Fakhruddinov³⁷, S. Falciano^{74a}, P. J. Falke²⁴, S. Falke³⁶, J. Faltova¹³², Y. Fan^{14a}, Y. Fang^{14a,14d}, G. Fanourakis⁴⁶, M. Fanti^{70a,70b}, M. Faraj^{68a,68b}, Z. Farazpay⁹⁶, A. Farbin⁸, A. Farilla^{76a}, T. Farooque¹⁰⁶, S. M. Farrington⁵², F. Fassi^{35e}, D. Fassouliotis⁹, M. Fauci Giannelli^{75a,75b}, W. J. Fawcett³², L. Fayard⁶⁶, P. Federicova¹³⁰, O. L. Fedin^{37,a}, G. Fedotov³⁷, M. Feickert¹⁶⁹, L. Felgioni¹⁰¹, A. Fell¹³⁸, D. E. Fellers¹²², C. Feng^{62b}, M. Feng^{14b}, Z. Feng¹¹³, M. J. Fenton¹⁵⁹, A. B. Fenyuk³⁷, L. Ferencz⁴⁸, J. Ferrando⁴⁸, A. Ferrari¹⁶⁰, P. Ferrari^{112,113}, R. Ferrari^{72a}, D. Ferrere⁵⁶, C. Ferretti¹⁰⁵, F. Fiedler⁹⁹, A. Filipčić⁹², E. K. Filmer¹, F. Filthaut¹¹², M. C. N. Fiolhais^{129a,129c}, L. Fiorini¹⁶², F. Fischer¹⁴⁰, W. C. Fisher¹⁰⁶, T. Fitschen¹⁰⁰, I. Fleck¹⁴⁰, P. Fleischmann¹⁰⁵, T. Flick¹⁷⁰, L. Flores¹²⁷, M. Flores^{33d,af}, L. R. Flores Castillo^{64a}, F. M. Follega^{77a,77b}, N. Fomin¹⁶, J. H. Foo¹⁵⁴, B. C. Forland⁶⁷, A. Formica¹³⁴, A. C. Forti¹⁰⁰, E. Fortin¹⁰¹, A. W. Fortman⁶¹, M. G. Foti^{17a}, L. Fountas^{9,k}, D. Fournier⁶⁶, H. Fox⁹⁰, P. Francavilla^{73a,73b}, S. Francescato⁶¹, S. Franchellucci⁵⁶, M. Franchini^{23a,23b}, S. Franchino^{63a}, D. Francis³⁶, L. Franco¹¹², L. Franconi¹⁹, M. Franklin⁶¹, G. Frattari²⁶, A. C. Freegard⁹³, P. M. Freeman²⁰, W. S. Freund^{81b}, N. Fritzsche⁵⁰, A. Froch⁵⁴, D. Froidevaux³⁶, J. A. Frost¹²⁵, Y. Fu^{62a}, M. Fujimoto¹¹⁷, E. Fullana Torregrosa^{162,*}, J. Fuster¹⁶², A. Gabrielli^{23a,23b}, A. Gabrielli¹⁵⁴, P. Gadow⁴⁸, G. Gagliardi^{57a,57b}, L. G. Gagnon^{17a}, G. E. Gallardo¹²⁵, E. J. Gallas¹²⁵, B. J. Gallop¹³³, R. Gamboa Goni⁹³, K. K. Gan¹¹⁸, S. Ganguly¹⁵², J. Gao^{62a}, Y. Gao⁵², F. M. Garay Walls^{136a,136b}, B. Garcia²⁹, C. García¹⁶², J. E. García Navarro¹⁶², J. A. García Pascual^{14a}, M. Garcia-Sciveres^{17a}, R. W. Gardner³⁹, D. Garg⁷⁹, R. B. Garg^{142,r}, S. Gargiulo⁵⁴, C. A. Garner¹⁵⁴, V. Garonne²⁹, S. J. Gasirowski¹³⁷, P. Gaspar^{81b}, G. Gaudio^{72a}, V. Gautam¹³, P. Gauzzi^{74a,74b}, I. L. Gavrilenko³⁷, A. Gavrilyuk³⁷, C. Gay¹⁶³, G. Gaycken⁴⁸, E. N. Gazis¹⁰, A. A. Geanta^{27b,27e}, C. M. Gee¹³⁵, J. Geisen⁹⁷, M. Geisen⁹⁹, C. Gemme^{57b}, M. H. Genest⁶⁰, S. Gentile^{74a,74b}, S. George⁹⁴, W. F. George²⁰, T. Gerialis⁴⁶, L. O. Gerlach⁵⁵, P. Gessinger-Befurt³⁶, M. Ghasemi Bostanabad¹⁶⁴, M. Ghneimat¹⁴⁰, K. Ghorbanian⁹³, A. Ghosal¹⁴⁰, A. Ghosh¹⁵⁹, A. Ghosh⁷, B. Giacobbe^{23b}, S. Giagu^{74a,74b}, N. Giangiacomi¹⁵⁴, P. Giannetti^{73a}, A. Giannini^{62a}, S. M. Gibson⁹⁴, M. Gignac¹³⁵, D. T. Gil^{84b}, A. K. Gilbert^{84a}, B. J. Gilbert⁴¹, D. Gillberg³⁴, G. Gilles¹¹³, N. E. K. Gillwald⁴⁸, L. Ginabat¹²⁶, D. M. Gingrich^{2,aj}, M. P. Giordani^{68a,68c}, P. F. Giraud¹³⁴, G. Giugliarelli^{68a,68c}, D. Giugni^{70a}, F. Giuli³⁶, I. Gkialas^{9,k}, L. K. Gladilin³⁷, C. Glasman⁹⁸, G. R. Gledhill¹²², M. Glisic¹²², I. Gnesi^{43b,g}, Y. Go^{29,am}, M. Goblirsch-Kolb²⁶, B. Gocke⁴⁹, D. Godin¹⁰⁷, S. Goldfarb¹⁰⁴, T. Golling⁵⁶, M. G. D. Gololo^{33g}, D. Golubkov³⁷, J. P. Gombas¹⁰⁶, A. Gomes^{129a,129b}, G. Gomes Da Silva¹⁴⁰, A. J. Gomez Delegido¹⁶², R. Goncalves Gama⁵⁵, R. Gonçalves^{129a,129c}, G. Gonella¹²², L. Gonella²⁰, A. Gongadze³⁸, F. Gonnella²⁰, J. L. Gonski⁴¹, R. Y. González Andana⁵², S. González de la Hoz¹⁶², S. Gonzalez Fernandez¹³, R. Gonzalez Lopez⁹¹, C. Gonzalez Renteria^{17a}, R. Gonzalez Suarez¹⁶⁰, S. Gonzalez-Sevilla⁵⁶, G. R. Gonzalvo Rodriguez¹⁶², L. Goossens³⁶, N. A. Gorasia²⁰, P. A. Gorbounov³⁷

D. P. Kisliuk¹⁵⁴, C. Kitsaki¹⁰, O. Kivernyk²⁴, M. Klassen^{63a}, C. Klein³⁴, L. Klein¹⁶⁵, M. H. Klein¹⁰⁵, M. Klein⁹¹, S. B. Klein⁵⁶, U. Klein⁹¹, P. Klimek³⁶, A. Klimentov²⁹, F. Klimpel¹⁰⁹, T. Klingl²⁴, T. Klioutchnikova³⁶, F. F. Klitzner¹⁰⁸, P. Kluit¹¹³, S. Kluth¹⁰⁹, E. Kneringer⁷⁸, T. M. Knight¹⁵⁴, A. Knue⁵⁴, D. Kobayashi⁸⁸, R. Kobayashi⁸⁶, M. Kocian¹⁴², P. Kodyš¹³², D. M. Koeck¹⁴⁵, P. T. Koenig²⁴, T. Koffas³⁴, M. Kolb¹³⁴, I. Koletsou⁴, T. Komarek¹²¹, K. Köneke⁵⁴, A. X. Y. Kong¹, T. Kono¹¹⁷, N. Konstantinidis⁹⁵, B. Konya⁹⁷, R. Kopeliansky⁶⁷, S. Koperny^{84a}, K. Korcyl⁸⁵, K. Kordas^{151.f}, G. Koren¹⁵⁰, A. Korn⁹⁵, S. Korn⁵⁵, I. Korolkov¹³, N. Korotkova³⁷, B. Kortman¹¹³, O. Kortner¹⁰⁹, S. Kortner¹⁰⁹, W. H. Kostecka¹¹⁴, V. V. Kostyukhin¹⁴⁰, A. Kotsokechagia¹³⁴, A. Kotwal⁵¹, A. Koulouris³⁶, A. Kourkoumeli-Charalampidi^{72a,72b}, C. Kourkoumelis⁹, E. Kourlitis⁶, O. Kovanda¹⁴⁵, R. Kowalewski¹⁶⁴, W. Kozanecki¹³⁴, A. S. Kozhin³⁷, V. A. Kramarenko³⁷, G. Kramberger⁹², P. Kramer⁹⁹, M. W. Krasny¹²⁶, A. Krasznahorkay³⁶, J. A. Kremer⁹⁹, T. Kresse⁵⁰, J. Kretzschmar⁹¹, K. Kreul¹⁸, P. Krieger¹⁵⁴, F. Krieter¹⁰⁸, S. Krishnamurthy¹⁰², A. Krishnan^{63b}, M. Krivos¹³², K. Krizka^{17a}, K. Kroeninger⁴⁹, H. Kroha¹⁰⁹, J. Kroll¹³⁰, J. Kroll¹²⁷, K. S. Krowpman¹⁰⁶, U. Kruchonak³⁸, H. Krüger²⁴, N. Krumnack⁸⁰, M. C. Kruse⁵¹, J. A. Krzysiak⁸⁵, O. Kuchinskaia³⁷, S. Kuday^{3a}, D. Kuechler⁴⁸, J. T. Kuechler⁴⁸, S. Kuehn³⁶, T. Kuhl⁴⁸, V. Kukhtin³⁸, Y. Kulchitsky^{37.a}, S. Kuleshov^{136b,136d}, M. Kumar^{33g}, N. Kumari¹⁰¹, A. Kupco¹³⁰, T. Kupfer⁴⁹, A. Kupich³⁷, O. Kuprash⁵⁴, H. Kurashige⁸³, L. L. Kurchaninov^{155a}, Y. A. Kurochkin³⁷, A. Kurova³⁷, M. Kuze¹⁵³, A. K. Kvam¹⁰², J. Kvita¹²¹, T. Kwan¹⁰³, K. W. Kwok^{64a}, N. G. Kyriacou¹⁰⁵, L. A. O. Laatu¹⁰¹, C. Lacasta¹⁶², F. Lacava^{74a,74b}, H. Lacker¹⁸, D. Lacour¹²⁶, N. N. Lad⁹⁵, E. Ladygin³⁸, B. Laforge¹²⁶, T. Lagouri^{136e}, S. Lai⁵⁵, I. K. Lakomic^{84a}, N. Lalloue⁶⁰, J. E. Lambert¹¹⁹, S. Lammers⁶⁷, W. Lampl⁷, C. Lampoudis^{151.f}, A. N. Lancaster¹¹⁴, E. Lançon²⁹, U. Landgraf⁵⁴, M. P. J. Landon⁹³, V. S. Lang⁵⁴, R. J. Langenberg¹⁰², A. J. Lankford¹⁵⁹, F. Lanni³⁶, K. Lantzsch²⁴, A. Lanza^{72a}, A. Lapertosa^{57a,57b}, J. F. Laporte¹³⁴, T. Lari^{70a}, F. Lasagni Manghi^{23b}, M. Lassnig³⁶, V. Latonova¹³⁰, T. S. Lau^{64a}, A. Laudrain⁹⁹, A. Laurier³⁴, S. D. Lawlor⁹⁴, Z. Lawrence¹⁰⁰, M. Lazzaroni^{70a,70b}, B. Le¹⁰⁰, B. Leban⁹², A. Lebedev⁸⁰, M. LeBlanc³⁶, T. LeCompte⁶, F. Ledroit-Guillon⁶⁰, A. C. A. Lee⁹⁵, G. R. Lee¹⁶, L. Lee⁶¹, S. C. Lee¹⁴⁷, S. Lee^{47a,47b}, T. F. Lee⁹¹, L. L. Leeuw^{33c}, H. P. Lefebvre⁹⁴, M. Lefebvre¹⁶⁴, C. Leggett^{17a}, K. Lehmann¹⁴¹, G. Lehmann Miotto³⁶, M. Leigh⁵⁶, W. A. Leight¹⁰², A. Leisos^{151.v}, M. A. L. Leite^{81c}, C. E. Leitgeb⁴⁸, R. Leitner¹³², K. J. C. Leney⁴⁴, T. Lenz²⁴, S. Leone^{73a}, C. Leonidopoulos⁵², A. Leopold¹⁴³, C. Leroy¹⁰⁷, R. Les¹⁰⁶, C. G. Lester³², M. Levchenko³⁷, J. Levêque⁴, D. Levin¹⁰⁵, L. J. Levinson¹⁶⁸, M. P. Lewicki⁸⁵, D. J. Lewis⁴, A. Li⁵, B. Li^{14b}, B. Li^{62b}, C. Li^{62a}, C-Q. Li^{62c}, H. Li^{62a}, H. Li^{62b}, H. Li^{14c}, H. Li^{62b}, J. Li^{62c}, K. Li¹³⁷, L. Li^{62c}, M. Li^{14a,14d}, Q. Y. Li^{62a}, S. Li^{14a,14d}, S. Li^{62d,62c,e}, T. Li^{62b}, X. Li¹⁰³, Z. Li^{62b}, Z. Li¹²⁵, Z. Li¹⁰³, Z. Li⁹¹, Z. Li^{14a,14d}, Z. Liang^{14a}, M. Liberatore⁴⁸, B. Liberti^{75a}, K. Lie^{64c}, J. Lieber Marin^{81b}, K. Lin¹⁰⁶, R. A. Linck⁶⁷, R. E. Lindley⁷, J. H. Lindon², A. Linss⁴⁸, E. Lipeles¹²⁷, A. Lipniacka¹⁶, A. Lister¹⁶³, J. D. Little⁴, B. Liu^{14a}, B. X. Liu¹⁴¹, D. Liu^{62d,62c}, J. B. Liu^{62a}, J. K. K. Liu³², K. Liu^{62d,62c}, M. Liu^{62a}, M. Y. Liu^{62a}, P. Liu^{14a}, Q. Liu^{62c,62d,137}, X. Liu^{62a}, Y. Liu⁴⁸, Y. Liu^{14c,14d}, Y. L. Liu¹⁰⁵, Y. W. Liu^{62a}, M. Livan^{72a,72b}, J. Llorente Merino¹⁴¹, S. L. Lloyd⁹³, E. M. Lobodzinska⁴⁸, P. Loch⁷, S. Loffredo^{75a,75b}, T. Lohse¹⁸, K. Lohwasser¹³⁸, M. Lokajicek^{130,*}, J. D. Long¹⁶¹, I. Longarini^{74a,74b}, L. Longo^{69a,69b}, R. Longo¹⁶¹, I. Lopez Paz³⁶, A. Lopez Solis⁴⁸, J. Lorenz¹⁰⁸, N. Lorenzo Martinez⁴, A. M. Lory¹⁰⁸, A. Lösle⁵⁴, X. Lou^{47a,47b}, X. Lou^{14a,14d}, A. Lounis⁶⁶, J. Love⁶, P. A. Love⁹⁰, J. J. Lozano Bahilo¹⁶², G. Lu^{14a,14d}, M. Lu⁷⁹, S. Lu¹²⁷, Y. J. Lu⁶⁵, H. J. Lubatti¹³⁷, C. Luci^{74a,74b}, F. L. Lucio Alves^{14c}, A. Lucotte⁶⁰, F. Luehring⁶⁷, I. Luise¹⁴⁴, O. Lukianchuk⁶⁶, O. Lundberg¹⁴³, B. Lund-Jensen¹⁴³, N. A. Luongo¹²², M. S. Lutz¹⁵⁰, D. Lynn²⁹, H. Lyons⁹¹, R. Lysak¹³⁰, E. Lytken⁹⁷, F. Lyu^{14a}, V. Lyubushkin³⁸, T. Lyubushkina³⁸, H. Ma²⁹, L. L. Ma^{62b}, Y. Ma⁹⁵, D. M. Mac Donell¹⁶⁴, G. Maccarrone⁵³, J. C. MacDonald¹³⁸, R. Madar⁴⁰, W. F. Mader⁵⁰, J. Maeda⁸³, T. Maeno²⁹, M. Maerker⁵⁰, V. Magerl⁵⁴, H. Maguire¹³⁸, D. J. Mahon⁴¹, C. Maidantchik^{81b}, A. Maio^{129a,129b,129d}, K. Maj^{84a}, O. Majersky^{28a}, S. Majewski¹²², N. Makovec⁶⁶, V. Maksimovic¹⁵, B. Malaescu¹²⁶, Pa. Malecki⁸⁵, V. P. Maleev³⁷, F. Malek⁶⁰, D. Malito^{43a,43b}, U. Mallik⁷⁹, C. Malone³², S. Maltezos¹⁰, S. Malyukov³⁸, J. Mamuzic¹³, G. Mancini⁵³, G. Manco^{72a,72b}, J. P. Mandalia⁹³, I. Mandić⁹², L. Manhaes de Andrade Filho^{81a}, I. M. Maniatis^{151.f}, M. Manisha¹³⁴, J. Manjarres Ramos⁵⁰, D. C. Mankad¹⁶⁸, A. Mann¹⁰⁸, B. Mansoulie¹³⁴, S. Manzoni³⁶, A. Marantis^{151.v}, G. Marchiori⁵, M. Marcisovsky¹³⁰, L. Marcoccia^{75a,75b}, C. Marcon^{70a}, M. Marinescu²⁰, M. Marjanovic¹¹⁹, E. J. Marshall⁹⁰, Z. Marshall^{17a}, S. Marti-Garcia¹⁶², T. A. Martin¹⁶⁶, V. J. Martin⁵², B. Martin dit Latour¹⁶, L. Martinelli^{74a,74b}, M. Martinez^{13.w}, P. Martinez Agullo¹⁶², V. I. Martinez Outschoorn¹⁰², P. Martinez Suarez¹³, S. Martin-Haugh¹³³, V. S. Martoiu^{27b}, A. C. Martyniuk⁹⁵, A. Marzin³⁶, S. R. Maschek¹⁰⁹, L. Masetti⁹⁹

T. Mashimo¹⁵², J. Masik¹⁰⁰, A. L. Maslennikov³⁷, L. Massa^{23b}, P. Massarotti^{71a,71b}, P. Mastrandrea^{73a,73b}, A. Mastroberardino^{43a,43b}, T. Masubuchi¹⁵², T. Mathisen¹⁶⁰, N. Matsuzawa¹⁵², J. Maurer^{27b}, B. Mačec⁹², D. A. Maximov³⁷, R. Mazini¹⁴⁷, I. Maznas^{151,f}, M. Mazza¹⁰⁶, S. M. Mazza¹³⁵, C. Mc Ginn²⁹, J. P. Mc Gowan¹⁰³, S. P. Mc Kee¹⁰⁵, W. P. McCormack^{17a}, E. F. McDonald¹⁰⁴, A. E. McDougall¹¹³, J. A. Mcfayden¹⁴⁵, G. Mchedlize^{148b}, R. P. Mckenzie^{33g}, T. C. Mclachlan⁴⁸, D. J. McLaughlin⁹⁵, K. D. McLean¹⁶⁴, S. J. McMahon¹³³, P. C. McNamara¹⁰⁴, C. M. Mcpartland⁹¹, R. A. McPherson^{164,z}, T. Megy⁴⁰, S. Mehlhase¹⁰⁸, A. Mehta⁹¹, B. Meirose⁴⁵, D. Melini¹⁴⁹, B. R. Mellado Garcia^{33g}, A. H. Melo⁵⁵, F. Meloni⁴⁸, E. D. Mendes Gouveia^{129a}, A. M. Mendes Jacques Da Costa²⁰, H. Y. Meng¹⁵⁴, L. Meng⁹⁰, S. Menke¹⁰⁹, M. Mentink³⁶, E. Meoni^{43a,43b}, C. Merlassino¹²⁵, L. Merola^{71a,71b}, C. Meroni^{70a,70b}, G. Merz¹⁰⁵, O. Meshkov³⁷, J. K. R. Meshreki¹⁴⁰, J. Metcalfe⁶, A. S. Mete⁶, C. Meyer⁶⁷, J-P. Meyer¹³⁴, M. Michetti¹⁸, R. P. Middleton¹³³, L. Mijović⁵², G. Mikenberg¹⁶⁸, M. Mikestikova¹³⁰, M. Mikuž⁹², H. Mildner¹³⁸, A. Milic³⁶, C. D. Milke⁴⁴, D. W. Miller³⁹, L. S. Miller³⁴, A. Milov¹⁶⁸, D. A. Milstead^{47a,47b}, T. Min^{14c}, A. A. Minaenko³⁷, I. A. Minashvili^{148b}, L. Mince⁵⁹, A. I. Mincer¹¹⁶, B. Mindur^{84a}, M. Mineev³⁸, Y. Mino⁸⁶, L. M. Mir¹³, M. Miralles Lopez¹⁶², M. Mironova¹²⁵, M. C. Missio¹¹², T. Mitani¹⁶⁷, A. Mitra¹⁶⁶, V. A. Mitsou¹⁶², O. Miu¹⁵⁴, P. S. Miyagawa⁹³, Y. Miyazaki⁸⁸, A. Mizukami⁸², J. U. Mjörnmark⁹⁷, T. Mkrtchyan^{63a}, T. Mlinarevic⁹⁵, M. Mlynarikova³⁶, T. Moa^{47a,47b}, S. Mobius⁵⁵, K. Mochizuki¹⁰⁷, P. Moder⁴⁸, P. Mogg¹⁰⁸, A. F. Mohammed^{14a,14d}, S. Mohapatra⁴¹, G. Mokgatitswane^{33g}, B. Mondal¹⁴⁰, S. Mondal¹³¹, K. Mönig⁴⁸, E. Monnier¹⁰¹, L. Monsonis Romero¹⁶², J. Montejo Berlingen³⁶, M. Montella¹¹⁸, F. Monticelli⁸⁹, N. Morange⁶⁶, A. L. Moreira De Carvalho^{129a}, M. Moreno Llácer¹⁶², C. Moreno Martinez⁵⁶, P. Moretini^{57b}, S. Morgenstern¹⁶⁶, M. Morii⁶¹, M. Morinaga¹⁵², A. K. Morley³⁶, F. Morodei^{74a,74b}, L. Morvaj³⁶, P. Moschovakos³⁶, B. Moser³⁶, M. Mosidze^{148b}, T. Moskalets⁵⁴, P. Moskvitina¹¹², J. Moss^{31,p}, E. J. W. Moyse¹⁰², O. Mtintsilana^{33g}, S. Muanza¹⁰¹, J. Mueller¹²⁸, D. Muenstermann⁹⁰, R. Müller¹⁹, G. A. Mullier¹⁶⁰, J. J. Mullin¹²⁷, D. P. Mungo¹⁵⁴, J. L. Munoz Martinez¹³, D. Munoz Perez¹⁶², F. J. Munoz Sanchez¹⁰⁰, M. Murin¹⁰⁰, W. J. Murray^{133,166}, A. Murrone^{70a,70b}, J. M. Muse¹¹⁹, M. Muškinja^{17a}, C. Mwewa²⁹, A. G. Myagkov^{37,a}, A. J. Myers⁸, A. A. Myers¹²⁸, G. Myers⁶⁷, M. Myska¹³¹, B. P. Nachman^{17a}, O. Nackenhorst⁴⁹, A. Nag⁵⁰, K. Nagai¹²⁵, K. Nagano⁸², J. L. Nagle^{29,am}, E. Nagy¹⁰¹, A. M. Nairz³⁶, Y. Nakahama⁸², K. Nakamura⁸², H. Nanjo¹²³, R. Narayan⁴⁴, E. A. Narayanan¹¹¹, I. Naryshkin³⁷, M. Naseri³⁴, C. Nass²⁴, G. Navarro^{22a}, J. Navarro-Gonzalez¹⁶², R. Nayak¹⁵⁰, A. Nayaz¹⁸, P. Y. Nechaeva³⁷, F. Nechansky⁴⁸, L. Nedic¹²⁵, T. J. Neep²⁰, A. Negri^{72a,72b}, M. Negrini^{23b}, C. Nellist¹¹², C. Nelson¹⁰³, K. Nelson¹⁰⁵, S. Nemecek¹³⁰, M. Nessi^{36,i}, M. S. Neubauer¹⁶¹, F. Neuhaus⁹⁹, J. Neundorf⁴⁸, R. Newhouse¹⁶³, P. R. Newman²⁰, C. W. Ng¹²⁸, Y. S. Ng¹⁸, Y. W. Y. Ng⁴⁸, B. Ngair^{35c}, H. D. N. Nguyen¹⁰⁷, R. B. Nickerson¹²⁵, R. Nicolaidou¹³⁴, J. Nielsen¹³⁵, M. Niemeyer⁵⁵, N. Nikiforou³⁶, V. Nikolaenko^{37,a}, I. Nikolic-Audit¹²⁶, K. Nikolopoulos²⁰, P. Nilsson²⁹, H. R. Nindhito⁵⁶, A. Nisati^{74a}, N. Nishu², R. Nisius¹⁰⁹, J-E. Nitschke⁵⁰, E. K. Nkadimeng^{33g}, S. J. Noacco Rosende⁸⁹, T. Nobe¹⁵², D. L. Noel³², Y. Noguchi⁸⁶, T. Nommensen¹⁴⁶, M. A. Nomura²⁹, M. B. Norfolk¹³⁸, R. R. B. Norisam⁹⁵, B. J. Norman³⁴, J. Novak⁹², T. Novak⁴⁸, O. Novgorodova⁵⁰, L. Novotny¹³¹, R. Novotny¹¹¹, L. Nozka¹²¹, K. Ntekas¹⁵⁹, N. M. J. Nunes De Moura Junior^{81b}, E. Nurse⁹⁵, F. G. Oakham^{34,aj}, J. Ocariz¹²⁶, A. Ochi⁸³, I. Ochoa^{129a}, S. Oerdek¹⁶⁰, A. Ogrodnik^{84a}, A. Oh¹⁰⁰, C. C. Ohm¹⁴³, H. Oide⁸², R. Oishi¹⁵², M. L. Ojeda⁴⁸, Y. Okazaki⁸⁶, M. W. O'Keefe⁹¹, Y. Okumura¹⁵², A. Olariu^{27b}, L. F. Oleiro Seabra^{129a}, S. A. Olivares Pino^{136e}, D. Oliveira Damazio²⁹, D. Oliveira Goncalves^{81a}, J. L. Oliver¹⁵⁹, M. J. R. Olsson¹⁵⁹, A. Olszewski⁸⁵, J. Olszowska^{85,*}, Ö. O. Öncel⁵⁴, D. C. O'Neil¹⁴¹, A. P. O'Neill¹⁹, A. Onofre^{129a,129e}, P. U. E. Onyisi¹¹, M. J. Oreglia³⁹, G. E. Orellana⁸⁹, D. Orestano^{76a,76b}, N. Orlando¹³, R. S. Orr¹⁵⁴, V. O'Shea⁵⁹, R. Ospanov^{62a}, G. Otero y Garzon³⁰, H. Otono⁸⁸, P. S. Ott^{63a}, G. J. Ottino^{17a}, M. Ouchrif^{35d}, J. Ouellette^{29,am}, F. Ould-Saada¹²⁴, M. Owen⁵⁹, R. E. Owen¹³³, K. Y. Oyulmaz^{21a}, V. E. Ozcan^{21a}, N. Ozturk⁸, S. Ozturk^{21d}, J. Pacalt¹²¹, H. A. Pacey³², A. Pacheco Pages¹³, C. Padilla Aranda¹³, G. Padovano^{74a,74b}, S. Pagan Griso^{17a}, G. Palacino⁶⁷, A. Palazzo^{69a,69b}, S. Palestini³⁶, M. Palka^{84b}, J. Pan¹⁷¹, T. Pan^{64a}, D. K. Panchal¹¹, C. E. Pandini¹¹³, J. G. Panduro Vazquez⁹⁴, H. Pang^{14b}, P. Pani⁴⁸, G. Panizzo^{68a,68c}, L. Paolozzi⁵⁶, C. Papadatos¹⁰⁷, S. Parajuli⁴⁴, A. Paramonov⁶, C. Paraskevopoulos¹⁰, D. Paredes Hernandez^{64b}, T. H. Park¹⁵⁴, M. A. Parker³², F. Parodi^{57a,57b}, E. W. Parrish¹¹⁴, V. A. Parrish⁵², J. A. Parsons⁴¹, U. Parzefall⁵⁴, B. Pascual Dias¹⁰⁷, L. Pascual Dominguez¹⁵⁰, V. R. Pascuzzi^{17a}, F. Pasquali¹¹³, E. Pasqualucci^{74a}, S. Passaggio^{57b}, F. Pastore⁹⁴, P. Pasuwan^{47a,47b}, P. Patel⁸⁵, J. R. Pater¹⁰⁰, T. Pauly³⁶, J. Parkes¹⁴², M. Pedersen¹²⁴, R. Pedro^{129a}, S. V. Peleganchuk³⁷, O. Penc³⁶, E. A. Pender⁵², C. Peng^{64b}, H. Peng^{62a}, K. E. Pensi¹⁰⁸, M. Penzin³⁷, B. S. Peralva^{81d}, A. P. Pereira Peixoto⁶⁰, L. Pereira Sanchez^{47a,47b}

D. V. Perepelitsa^{29,am}, E. Perez Codina^{155a}, M. Perganti¹⁰, L. Perini^{70a,70b,*}, H. Pernegger³⁶, A. Perrevoort¹¹², O. Perrin⁴⁰, K. Peters⁴⁸, R. F. Y. Peters¹⁰⁰, B. A. Petersen³⁶, T. C. Petersen⁴², E. Petit¹⁰¹, V. Petousis¹³¹, C. Petridou^{151,f}, A. Petrukhin¹⁴⁰, M. Pettee^{17a}, N. E. Pettersson³⁶, A. Petukhov³⁷, K. Petukhova¹³², A. Peyaud¹³⁴, R. Pezoa^{136f}, L. Pezzotti³⁶, G. Pezzullo¹⁷¹, T. M. Pham¹⁶⁹, T. Pham¹⁰⁴, P. W. Phillips¹³³, M. W. Phipps¹⁶¹, G. Piacquadio¹⁴⁴, E. Pianori^{17a}, F. Piazza^{70a,70b}, R. Piegai³⁰, D. Pietreanu^{27b}, A. D. Pilkington¹⁰⁰, M. Pinamonti^{68a,68c}, J. L. Pinfeld², B. C. Pinheiro Pereira^{129a}, C. Pitman Donaldson⁹⁵, D. A. Pizzi³⁴, L. Pizzimento^{75a,75b}, A. Pizzini¹¹³, M.-A. Pleier²⁹, V. Plesanovs⁵⁴, V. Pleskot¹³², E. Plotnikova³⁸, G. Poddar⁴, R. Poettgen⁹⁷, L. Poggioli¹²⁶, I. Pogrebnyak¹⁰⁶, D. Pohl²⁴, I. Pokharel⁵⁵, S. Polacek¹³², G. Polesello^{72a}, A. Poley^{141,155a}, R. Polifka¹³¹, A. Polini^{23b}, C. S. Pollard¹²⁵, Z. B. Pollock¹¹⁸, V. Polychronakos²⁹, E. Pompa Pacchi^{74a,74b}, D. Ponomarenko³⁷, L. Pontecorvo³⁶, S. Popa^{27a}, G. A. Popeneciu^{27d}, D. M. Portillo Quintero^{155a}, S. Pospisil¹³¹, P. Postolache^{27c}, K. Potamianos¹²⁵, I. N. Potrap³⁸, C. J. Potter³², H. Potti¹, T. Poulsen⁴⁸, J. Poveda¹⁶², M. E. Pozo Astigarraga³⁶, A. Prades Ibanez¹⁶², M. M. Prapa⁴⁶, J. Pretel⁵⁴, D. Price¹⁰⁰, M. Primavera^{69a}, M. A. Principe Martin⁹⁸, R. Privara¹²¹, M. L. Proffitt¹³⁷, N. Proklova¹²⁷, K. Prokofiev^{64c}, G. Proto^{75a,75b}, S. Protopopescu²⁹, J. Proudfoot⁶, M. Przybycien^{84a}, J. E. Puddefoot¹³⁸, D. Pudzha³⁷, P. Puzo⁶⁶, D. Pyatiizbyantseva³⁷, J. Qian¹⁰⁵, D. Qichen¹⁰⁰, Y. Qin¹⁰⁰, T. Qiu⁹³, A. Quadt⁵⁵, M. Queitsch-Maitland¹⁰⁰, G. Quetant⁵⁶, G. Rabanal Bolanos⁶¹, D. Rafanoharana⁵⁴, F. Ragusa^{70a,70b}, J. L. Rainbolt³⁹, J. A. Raine⁵⁶, S. Rajagopalan²⁹, E. Ramakoti³⁷, K. Ran^{14d,48}, N. P. Rapheeha^{33g}, V. Raskina¹²⁶, D. F. Rassloff^{63a}, S. Rave⁹⁹, B. Ravina⁵⁵, I. Ravinovich¹⁶⁸, M. Raymond³⁶, A. L. Read¹²⁴, N. P. Readioff¹³⁸, D. M. Rebutti^{72a,72b}, G. Redlinger²⁹, K. Reeves⁴⁵, J. A. Reidelsturz¹⁷⁰, D. Reikher¹⁵⁰, A. Reiss⁹⁹, A. Rej¹⁴⁰, C. Rembser³⁶, A. Renardi⁴⁸, M. Renda^{27b}, M. B. Rendel¹⁰⁹, F. Renner⁴⁸, A. G. Rennie⁵⁹, S. Resconi^{70a}, M. Ressegotti^{57a,57b}, E. D. Resseguie^{17a}, S. Rettie³⁶, J. G. Reyes Rivera¹⁰⁶, B. Reynolds¹¹⁸, E. Reynolds^{17a}, M. Rezaei Estabragh¹⁷⁰, O. L. Rezanova³⁷, P. Reznicek¹³², E. Ricci^{77a,77b}, R. Richter¹⁰⁹, S. Richter^{47a,47b}, E. Richter-Was^{84b}, M. Ridel¹²⁶, P. Rieck¹¹⁶, P. Riedler³⁶, M. Rijssenbeek¹⁴⁴, A. Rimoldi^{72a,72b}, M. Rimoldi⁴⁸, L. Rinaldi^{23a,23b}, T. T. Rinn²⁹, M. P. Rinnagel¹⁰⁸, G. Ripellino¹⁴³, I. Riu¹³, P. Rivadeneira⁴⁸, J. C. Rivera Vergara¹⁶⁴, F. Rizatdinova¹²⁰, E. Rizvi⁹³, C. Rizzi⁵⁶, B. A. Roberts¹⁶⁶, B. R. Roberts^{17a}, S. H. Robertson^{103,z}, M. Robin⁴⁸, D. Robinson³², C. M. Robles Gajardo^{136f}, M. Robles Manzano⁹⁹, A. Robson⁵⁹, A. Rocchi^{75a,75b}, C. Roda^{73a,73b}, S. Rodriguez Bosca^{63a}, Y. Rodriguez Garcia^{22a}, A. Rodriguez Rodriguez⁵⁴, A. M. Rodríguez Vera^{155b}, S. Roe³⁶, J. T. Roemer¹⁵⁹, A. R. Roepe-Gier¹¹⁹, J. Roggel¹⁷⁰, O. Röhne¹²⁴, R. A. Rojas¹⁶⁴, B. Roland⁵⁴, C. P. A. Roland⁶⁷, J. Roloff²⁹, A. Romaniouk³⁷, E. Romano^{72a,72b}, M. Romano^{23b}, A. C. Romero Hernandez¹⁶¹, N. Rompotis⁹¹, L. Roos¹²⁶, S. Rosati^{74a}, B. J. Rosser³⁹, E. Rossi⁴, E. Rossi^{71a,71b}, L. P. Rossi^{57b}, L. Rossini⁴⁸, R. Rosten¹¹⁸, M. Rotaru^{27b}, B. Rottler⁵⁴, D. Rousseau⁶⁶, D. Rouso³², G. Rovelli^{72a,72b}, A. Roy¹⁶¹, A. Rozanov¹⁰¹, Y. Rozen¹⁴⁹, X. Ruan^{33g}, A. Rubio Jimenez¹⁶², A. J. Ruby⁹¹, V. H. Ruelas Rivera¹⁸, T. A. Ruggeri¹, F. Rühr⁵⁴, A. Ruiz-Martinez¹⁶², A. Rummler³⁶, Z. Rurikova⁵⁴, N. A. Rusakovich³⁸, H. L. Russell¹⁶⁴, J. P. Rutherford⁷, K. Rybacki⁹⁰, M. Rybar¹³², E. B. Rye¹²⁴, A. Ryzhov³⁷, J. A. Sabater Iglesias⁵⁶, P. Sabatini¹⁶², L. Sabetta^{74a,74b}, H. F.-W. Sadrozinski¹³⁵, F. Safai Tehrani^{74a}, B. Safarzadeh Samani¹⁴⁵, M. Safdari¹⁴², S. Saha¹⁰³, M. Sahinsky¹⁰⁹, M. Saimpert¹³⁴, M. Saito¹⁵², T. Saito¹⁵², D. Salamani³⁶, G. Salamanna^{76a,76b}, A. Salnikov¹⁴², J. Salt¹⁶², A. Salvador Salas¹³, D. Salvatore^{43a,43b}, F. Salvatore¹⁴⁵, A. Salzburger³⁶, D. Sammel⁵⁴, D. Sampsonidis^{151,f}, D. Sampsonidou^{62d,62c}, J. Sánchez¹⁶², A. Sanchez Pineda⁴, V. Sanchez Sebastian¹⁶², H. Sandaker¹²⁴, C. O. Sander⁴⁸, J. A. Sandesara¹⁰², M. Sandhoff¹⁷⁰, C. Sandoval^{22b}, D. P. C. Sankey¹³³, A. Sansoni⁵³, L. Santi^{74a,74b}, C. Santoni⁴⁰, H. Santos^{129a,129b}, S. N. Santpur^{17a}, A. Santra¹⁶⁸, K. A. Saoucha¹³⁸, J. G. Saraiva^{129a,129d}, J. Sardain⁷, O. Sasaki⁸², K. Sato¹⁵⁶, C. Sauer^{63b}, F. Sauerburger⁵⁴, E. Sauvan⁴, P. Savard^{154,aj}, R. Sawada¹⁵², C. Sawyer¹³³, L. Sawyer⁹⁶, I. Sayago Galvan¹⁶², C. Sbarra^{23b}, A. Sbrizzi^{23a,23b}, T. Scanlon⁹⁵, J. Schaarschmidt¹³⁷, P. Schacht¹⁰⁹, D. Schaefer³⁹, U. Schäfer⁹⁹, A. C. Schaffer⁶⁶, D. Schaile¹⁰⁸, R. D. Schamberger¹⁴⁴, E. Schanet¹⁰⁸, C. Scharf¹⁸, M. M. Schefer¹⁹, V. A. Schegelsky³⁷, D. Scheirich¹³², F. Schenck¹⁸, M. Schernau¹⁵⁹, C. Scheulen⁵⁵, C. Schiavi^{57a,57b}, Z. M. Schillaci²⁶, E. J. Schioppa^{69a,69b}, M. Schioppa^{43a,43b}, B. Schlag⁹⁹, K. E. Schleicher⁵⁴, S. Schlenker³⁶, J. Schmeing¹⁷⁰, M. A. Schmidt¹⁷⁰, K. Schmieden⁹⁹, C. Schmitt⁹⁹, S. Schmitt⁴⁸, L. Schoeffel¹³⁴, A. Schoening^{63b}, P. G. Scholer⁵⁴, E. Schopf¹²⁵, M. Schott⁹⁹, J. Schovancova³⁶, S. Schramm⁵⁶, F. Schroeder¹⁷⁰, H.-C. Schultz-Coulon^{63a}, M. Schumacher⁵⁴, B. A. Schumm¹³⁵, Ph. Schune¹³⁴, A. Schwartzman¹⁴², T. A. Schwarz¹⁰⁵, Ph. Schwemling¹³⁴, R. Schwienhorst¹⁰⁶, A. Sciandra¹³⁵, G. Sciolla²⁶, F. Scuri^{73a}, F. Scutti¹⁰⁴, C. D. Sebastiani⁹¹, K. Sedlaczek⁴⁹, P. Seema¹⁸, S. C. Seidel¹¹¹, A. Seiden¹³⁵

B. D. Seidlitz⁴¹, T. Seiss³⁹, C. Seitz⁴⁸, J. M. Seixas^{81b}, G. Sekhniaidze^{71a}, S. J. Sekula⁴⁴, L. Selem⁴, N. Semprini-Cesari^{23a,23b}, S. Sen⁵¹, D. Sengupta⁵⁶, V. Senthilkumar¹⁶², L. Serin⁶⁶, L. Serkin^{68a,68b}, M. Sessa^{76a,76b}, H. Severini¹¹⁹, S. Sevova¹⁴², F. Sforza^{57a,57b}, A. Sfyrlla⁵⁶, E. Shabalina⁵⁵, R. Shaheen¹⁴³, J. D. Shahinian¹²⁷, D. Shaked Renous¹⁶⁸, L. Y. Shan^{14a}, M. Shapiro^{17a}, A. Sharma³⁶, A. S. Sharma¹⁶³, P. Sharma⁷⁹, S. Sharma⁴⁸, P. B. Shatalov³⁷, K. Shaw¹⁴⁵, S. M. Shaw¹⁰⁰, Q. Shen^{5.62c}, P. Sherwood⁹⁵, L. Shi⁹⁵, C. O. Shimmin¹⁷¹, Y. Shimogama¹⁶⁷, J. D. Shinner⁹⁴, I. P. J. Shipsey¹²⁵, S. Shirabe⁶⁰, M. Shiyakova^{38.y}, J. Shlomi¹⁶⁸, M. J. Shochet³⁹, J. Shojaii¹⁰⁴, D. R. Shope¹²⁴, S. Shrestha^{118.an}, E. M. Shrif^{33g}, M. J. Shroff¹⁶⁴, P. Sicho¹³⁰, A. M. Sickles¹⁶¹, E. Sideras Haddad^{33g}, A. Sidoti^{23b}, F. Siegert⁵⁰, Dj. Sijacki¹⁵, R. Sikora^{84a}, F. Sili⁸⁹, J. M. Silva²⁰, M. V. Silva Oliveira³⁶, S. B. Silverstein^{47a}, S. Simion⁶⁶, R. Simoniello³⁶, E. L. Simpson⁵⁹, N. D. Simpson⁹⁷, S. Simsek^{21d}, S. Sindhu⁵⁵, P. Sinervo¹⁵⁴, V. Sinetckii³⁷, S. Singh¹⁴¹, S. Singh¹⁵⁴, S. Sinha⁴⁸, S. Sinha^{33g}, M. Sioli^{23a,23b}, I. Siral³⁶, S. Yu. Sivoklov^{37,*}, J. Sjölin^{47a,47b}, A. Skaf⁵⁵, E. Skorda⁹⁷, P. Skubic¹¹⁹, M. Slawinska⁸⁵, V. Smakhtin¹⁶⁸, B. H. Smart¹³³, J. Smiesko³⁶, S. Yu. Smirnov³⁷, Y. Smirnov³⁷, L. N. Smirnova^{37.a}, O. Smirnova⁹⁷, A. C. Smith⁴¹, E. A. Smith³⁹, H. A. Smith¹²⁵, J. L. Smith⁹¹, R. Smith¹⁴², M. Smizanska⁹⁰, K. Smolek¹³¹, A. Smykiewicz⁸⁵, A. A. Snesarev³⁷, H. L. Snoek¹¹³, S. Snyder²⁹, R. Sobie^{164.z}, A. Soffer¹⁵⁰, C. A. Solans Sanchez³⁶, E. Yu. Soldatov³⁷, U. Soldevila¹⁶², A. A. Solodkov³⁷, S. Solomon⁵⁴, A. Soloshenko³⁸, K. Solovieva⁵⁴, O. V. Solovyanov³⁷, V. Solovyevev³⁷, P. Sommer³⁶, A. Sonay¹³, W. Y. Song^{155b}, A. Sopczak¹³¹, A. L. Sopio⁹⁵, F. Sopkova^{28b}, V. Sothilingam^{63a}, S. Sottocornola^{72a,72b}, R. Soualah^{115b}, Z. Soumami^{35c}, D. South⁴⁸, S. Spagnolo^{69a,69b}, M. Spalla¹⁰⁹, F. Spano⁹⁴, D. Sperlich⁵⁴, G. Spigo³⁶, M. Spina¹⁴⁵, S. Spinali⁹⁰, D. P. Spiteri⁵⁹, M. Spousta¹³², E. J. Staats³⁴, A. Stabile^{70a,70b}, R. Stamen^{63a}, M. Stamenkovic¹¹³, A. Stampekis²⁰, M. Standke²⁴, E. Stanecka⁸⁵, M. V. Stange⁵⁰, B. Stanislaus^{17a}, M. M. Stanitzki⁴⁸, M. Stankaityte¹²⁵, B. Stapf⁴⁸, E. A. Starchenko³⁷, G. H. Stark¹³⁵, J. Stark^{101.ad}, D. M. Starko^{155b}, P. Staroba¹³⁰, P. Starovoitov^{63a}, S. Stärz¹⁰³, R. Staszewski⁸⁵, G. Stavropoulos⁴⁶, J. Steentoft¹⁶⁰, P. Steinberg²⁹, A. L. Steinhebel¹²², B. Stelzer^{141,155a}, H. J. Stelzer¹²⁸, O. Stelzer-Chilton^{155a}, H. Stenzel⁵⁸, T. J. Stevenson¹⁴⁵, G. A. Stewart³⁶, M. C. Stockton³⁶, G. Stoica^{27b}, M. Stolarski^{129a}, S. Stonjek¹⁰⁹, A. Straessner⁵⁰, J. Strandberg¹⁴³, S. Strandberg^{47a,47b}, M. Strauss¹¹⁹, T. Strebler¹⁰¹, P. Strizenecek^{28b}, R. Ströhmer¹⁶⁵, D. M. Strom¹²², L. R. Strom⁴⁸, R. Stroynowski⁴⁴, A. Strubig^{47a,47b}, S. A. Stucci²⁹, B. Stugu¹⁶, J. Stupak¹¹⁹, N. A. Styles⁴⁸, D. Su¹⁴², S. Su^{62a}, W. Su^{62c,62d,137}, X. Su^{62a,66}, K. Sugizaki¹⁵², V. V. Sulini³⁷, M. J. Sullivan⁹¹, D. M. S. Sultan^{77a,77b}, L. Sultanaliev³⁷, S. Sultansoy^{3b}, T. Sumida⁸⁶, S. Sun¹⁰⁵, S. Sun¹⁶⁹, O. Sunneborn Gudnadottir¹⁶⁰, M. R. Sutton¹⁴⁵, M. Svatos¹³⁰, M. Swiatkowski^{155a}, T. Swirski¹⁶⁵, I. Sykora^{28a}, M. Sykora¹³², T. Sykora¹³², D. Ta⁹⁹, K. Tackmann^{48.x}, A. Taffard¹⁵⁹, R. Tafirout^{155a}, J. S. Tafoya Vargas⁶⁶, R. H. M. Taibah¹²⁶, R. Takashima⁸⁷, K. Takeda⁸³, E. P. Takeva⁵², Y. Takubo⁸², M. Talby¹⁰¹, A. A. Talyshchev³⁷, K. C. Tam^{64b}, N. M. Tamir¹⁵⁰, A. Tanaka¹⁵², J. Tanaka¹⁵², R. Tanaka⁶⁶, M. Tanasini^{57a,57b}, J. Tang^{62c}, Z. Tao¹⁶³, S. Tapia Araya⁸⁰, S. Tapprogge⁹⁹, A. Tarek Abouelfadl Mohamed¹⁰⁶, S. Tarem¹⁴⁹, K. Tariq^{62b}, G. Tarna^{27b,101}, G. F. Tartarelli^{70a}, P. Tas¹³², M. Tasevsky¹³⁰, E. Tassi^{43a,43b}, A. C. Tate¹⁶¹, G. Tateno¹⁵², Y. Tayalati^{35e}, G. N. Taylor¹⁰⁴, W. Taylor^{155b}, H. Teagle⁹¹, A. S. Tee¹⁶⁹, R. Teixeira De Lima¹⁴², P. Teixeira-Dias⁹⁴, J. J. Teoh¹⁵⁴, K. Terashi¹⁵², J. Terron⁹⁸, S. Terzo¹³, M. Testa⁵³, R. J. Teuscher^{154.z}, A. Thaler⁷⁸, O. Theiner⁵⁶, N. Themistokleous⁵², T. Thevenaux-Pelzer¹⁸, O. Thielmann¹⁷⁰, D. W. Thomas⁹⁴, J. P. Thomas²⁰, E. A. Thompson⁴⁸, P. D. Thompson²⁰, E. Thomson¹²⁷, E. J. Thorpe⁹³, Y. Tian⁵⁵, V. Tikhomirov^{37.a}, Yu. A. Tikhonov³⁷, S. Timoshenko³⁷, E. X. L. Ting¹, P. Tipton¹⁷¹, S. Tisserant¹⁰¹, S. H. Tlou^{33g}, A. Tmourji⁴⁰, K. Todome^{23a,23b}, S. Todorova-Nova¹³², S. Todt⁵⁰, M. Togawa⁸², J. Tojo⁸⁸, S. Tokár^{28a}, K. Tokushuku⁸², R. Tombs³², M. Tomoto^{82,110}, L. Tompkins^{142.r}, K. W. Topolnicki^{84b}, P. Tornambe¹⁰², E. Torrence¹²², H. Torres⁵⁰, E. Torró Pastor¹⁶², M. Toscani³⁰, C. Toscirri³⁹, M. Tost¹¹, D. R. Tovey¹³⁸, A. Traeet¹⁶, I. S. Trandafir^{27b}, T. Trefzger¹⁶⁵, A. Tricoli²⁹, I. M. Trigger^{155a}, S. Trincaz-Duvoid¹²⁶, D. A. Trischuk²⁶, B. Trocme⁶⁰, A. Trofymov⁶⁶, C. Troncon^{70a}, L. Truong^{33c}, M. Trzebinski⁸⁵, A. Trzupek⁸⁵, F. Tsai¹⁴⁴, M. Tsai¹⁰⁵, A. Tsiamis^{151.f}, P. V. Tsiareshka³⁷, S. Tsigaridas^{155a}, A. Tsirigotis^{151.v}, V. Tsiskaridze¹⁴⁴, E. G. Tskhadadze^{148a}, M. Tsopoulou^{151.f}, Y. Tsujikawa⁸⁶, I. I. Tsukerman³⁷, V. Tsulaia^{17a}, S. Tsuno⁸², O. Tsur¹⁴⁹, D. Tsybychev¹⁴⁴, Y. Tu^{64b}, A. Tudorache^{27b}, V. Tudorache^{27b}, A. N. Tuna³⁶, S. Turchikhin³⁸, I. Turk Cakir^{3a}, R. Turra^{70a}, T. Turtuvshin^{38.aa}, P. M. Tuts⁴¹, S. Tzamarias^{151.f}, P. Tzanis¹⁰, E. Tzovara⁹⁹, K. Uchida¹⁵², F. Ukegawa¹⁵⁶, P. A. Ulloa Poblete^{136c}, E. N. Umaka⁸⁰, G. Unal³⁶, M. Unal¹¹, A. Undrus²⁹, G. Unel¹⁵⁹, J. Urban^{28b}, P. Urquijo¹⁰⁴, G. Usai⁸, R. Ushioda¹⁵³, M. Usman¹⁰⁷, Z. Uysal^{21b}, L. Vacavant¹⁰¹, V. Vacek¹³¹, B. Vachon¹⁰³, K. O. H. Vadla¹²⁴, T. Vafeiadis³⁶, A. Vaitkus⁹⁵, C. Valderanis¹⁰⁸, E. Valdes Santurio^{47a,47b}

M. Valente^{155a}, S. Valentinetti^{23a,23b}, A. Valero¹⁶², A. Vallier^{101,ad}, J. A. Valls Ferrer¹⁶², T. R. Van Daalen¹³⁷, P. Van Gemmeren⁶, M. Van Rijnbach^{36,124}, S. Van Stroud⁹⁵, I. Van Vulpen¹¹³, M. Vanadia^{75a,75b}, W. Vandelli³⁶, M. Vandenbroucke¹³⁴, E. R. Vandewall¹²⁰, D. Vannicola¹⁵⁰, L. Vannoli^{57a,57b}, R. Vari^{74a}, E. W. Varnes⁷, C. Varni^{17a}, T. Varol¹⁴⁷, D. Varouchas⁶⁶, L. Varriale¹⁶², K. E. Varvell¹⁴⁶, M. E. Vasile^{27b}, L. Vaslin⁴⁰, G. A. Vasquez¹⁶⁴, F. Vazeille⁴⁰, T. Vazquez Schroeder³⁶, J. Veatch³¹, V. Vecchio¹⁰⁰, M. J. Veen¹⁰², I. Veliscek¹²⁵, L. M. Veloce¹⁵⁴, F. Veloso^{129a,129c}, S. Veneziano^{74a}, A. Ventura^{69a,69b}, A. Verbytskyi¹⁰⁹, M. Verducci^{73a,73b}, C. Vergis²⁴, M. Verissimo De Araujo^{81b}, W. Verkerke¹¹³, J. C. Vermeulen¹¹³, C. Vernieri¹⁴², P. J. Verschuuren⁹⁴, M. Vessella¹⁰², M. C. Vetterli^{141,aj}, A. Vgenopoulos^{151,f}, N. Viaux Maira^{136f}, T. Vickey¹³⁸, O. E. Vickey Boeriu¹³⁸, G. H. A. Viehhauser¹²⁵, L. Vigani^{63b}, M. Villa^{23a,23b}, M. Villaplana Perez¹⁶², E. M. Villhauer⁵², E. Vilucchi⁵³, M. G. Vincter³⁴, G. S. Virdee²⁰, A. Vishwakarma⁵², C. Vittori^{23a,23b}, I. Vivarelli¹⁴⁵, V. Vladimirov¹⁶⁶, E. Voevodina¹⁰⁹, F. Vogel¹⁰⁸, P. Vokac¹³¹, J. Von Ahnen⁴⁸, E. Von Toerne²⁴, B. Vormwald³⁶, V. Vorobel¹³², K. Vorobev³⁷, M. Vos¹⁶², J. H. Vosseveld⁹¹, M. Vozak¹¹³, L. Vozdecky⁹³, N. Vranjes¹⁵, M. Vranjes Milosavljevic¹⁵, M. Vreeswijk¹¹³, R. Vuillermet³⁶, O. Vujanovic⁹⁹, I. Vukotic³⁹, S. Wada¹⁵⁶, C. Wagner¹⁰², W. Wagner¹⁷⁰, S. Wahdan¹⁷⁰, H. Wahlberg⁸⁹, R. Wakasa¹⁵⁶, M. Wakida¹¹⁰, V. M. Walbrecht¹⁰⁹, J. Walder¹³³, R. Walker¹⁰⁸, W. Walkowiak¹⁴⁰, A. M. Wang⁶¹, A. Z. Wang¹⁶⁹, C. Wang^{62a}, C. Wang^{62c}, H. Wang^{17a}, J. Wang^{64a}, R. J. Wang⁹⁹, R. Wang⁶¹, R. Wang⁶, S. M. Wang¹⁴⁷, S. Wang^{62b}, T. Wang^{62a}, W. T. Wang⁷⁹, X. Wang^{14c}, X. Wang¹⁶¹, X. Wang^{62c}, Y. Wang^{62d}, Y. Wang^{14c}, Z. Wang¹⁰⁵, Z. Wang^{51,62c,62d}, Z. Wang¹⁰⁵, A. Warburton¹⁰³, R. J. Ward²⁰, N. Warrack⁵⁹, A. T. Watson²⁰, H. Watson⁵⁹, M. F. Watson²⁰, G. Watts¹³⁷, B. M. Waugh⁹⁵, A. F. Webb¹¹, C. Weber²⁹, H. A. Weber¹⁸, M. S. Weber¹⁹, S. M. Weber^{63a}, C. Wei^{62a}, Y. Wei¹²⁵, A. R. Weidberg¹²⁵, J. Weingarten⁴⁹, M. Weirich⁹⁹, C. Weiser⁵⁴, C. J. Wells⁴⁸, T. Wenaus²⁹, B. Wendland⁴⁹, T. Wengler³⁶, N. S. Wenke¹⁰⁹, N. Wermes²⁴, M. Wessels^{63a}, K. Whalen¹²², A. M. Wharton⁹⁰, A. S. White⁶¹, A. White⁸, M. J. White¹, D. Whiteson¹⁵⁹, L. Wickremasinghe¹²³, W. Wiedenmann¹⁶⁹, C. Wiel⁵⁰, M. Wielers¹³³, N. Wieseotte⁹⁹, C. Wiglesworth⁴², L. A. M. Wiik-Fuchs⁵⁴, D. J. Wilbern¹¹⁹, H. G. Wilkens³⁶, D. M. Williams⁴¹, H. H. Williams¹²⁷, S. Williams³², S. Willocq¹⁰², P. J. Windischhofer¹²⁵, F. Winklmeier¹²², B. T. Winter⁵⁴, J. K. Winter¹⁰⁰, M. Wittgen¹⁴², M. Wobisch⁹⁶, R. Wölker¹²⁵, J. Wollrath¹⁵⁹, M. W. Wolter⁸⁵, H. Wolters^{129a,129c}, V. W. S. Wong¹⁶³, A. F. Wongel⁴⁸, S. D. Worm⁴⁸, B. K. Wosiek⁸⁵, K. W. Woźniak⁸⁵, K. Wraight⁵⁹, J. Wu^{14a,14d}, M. Wu^{64a}, M. Wu¹¹², S. L. Wu¹⁶⁹, X. Wu⁵⁶, Y. Wu^{62a}, Z. Wu^{134,62a}, J. Wuerzinger¹²⁵, T. R. Wyatt¹⁰⁰, B. M. Wynne⁵², S. Xella⁴², L. Xia^{14c}, M. Xia^{14b}, J. Xiang^{64c}, X. Xiao¹⁰⁵, M. Xie^{62a}, X. Xie^{62a}, S. Xin^{14a,14d}, J. Xiong^{17a}, I. Xiotidis¹⁴⁵, D. Xu^{14a}, H. Xu^{62a}, H. Xu^{62a}, L. Xu^{62a}, R. Xu¹²⁷, T. Xu¹⁰⁵, W. Xu¹⁰⁵, Y. Xu^{14b}, Z. Xu^{62b}, Z. Xu^{14a}, B. Yabsley¹⁴⁶, S. Yacoub^{33a}, N. Yamaguchi⁸⁸, Y. Yamaguchi¹⁵³, H. Yamauchi¹⁵⁶, T. Yamazaki^{17a}, Y. Yamazaki⁸³, J. Yan^{62c}, S. Yan¹²⁵, Z. Yan²⁵, H. J. Yang^{62c,62d}, H. T. Yang^{62a}, S. Yang^{62a}, T. Yang^{64c}, X. Yang^{62a}, X. Yang^{14a}, Y. Yang⁴⁴, Z. Yang^{62a,105}, W-M. Yao^{17a}, Y. C. Yap⁴⁸, H. Ye^{14c}, H. Ye⁵⁵, J. Ye⁴⁴, S. Ye²⁹, X. Ye^{62a}, Y. Yeh⁹⁵, I. Yeletsikh³⁸, B. K. Yeo^{17a}, M. R. Yexley⁹⁰, P. Yin⁴¹, K. Yorita¹⁶⁷, S. Younas^{27b}, C. J. S. Young⁵⁴, C. Young¹⁴², M. Yuan¹⁰⁵, R. Yuan^{62b,1}, L. Yue⁹⁵, X. Yue^{63a}, M. Zaazoua^{35e}, B. Zabinski⁸⁵, E. Zaid⁵², T. Zakareishvili^{148b}, N. Zakharchuk³⁴, S. Zambito⁵⁶, J. A. Zamora Saa^{136b,136d}, J. Zang¹⁵², D. Zanzi⁵⁴, O. Zaplatilek¹³¹, S. V. ZeiBner⁴⁹, C. Zeitnitz¹⁷⁰, J. C. Zeng¹⁶¹, D. T. Zenger Jr²⁶, O. Zenin³⁷, T. Ženiš^{28a}, S. Zenz⁹³, S. Zerradi^{35a}, D. Zerwas⁶⁶, V. Zhabin³⁷, B. Zhang^{14c}, D. F. Zhang¹³⁸, G. Zhang^{14b}, J. Zhang^{62b}, J. Zhang⁶, K. Zhang^{14a,14d}, L. Zhang^{14c}, P. Zhang^{14a,14d}, R. Zhang¹⁶⁹, S. Zhang¹⁰⁵, T. Zhang¹⁵², X. Zhang^{62c}, X. Zhang^{62b}, Y. Zhang^{5,62c}, Z. Zhang^{17a}, Z. Zhang⁶⁶, H. Zhao¹³⁷, P. Zhao⁵¹, T. Zhao^{62b}, Y. Zhao¹³⁵, Z. Zhao^{62a}, A. Zhemchugov³⁸, X. Zheng^{62a}, Z. Zheng¹⁴², D. Zhong¹⁶¹, B. Zhou¹⁰⁵, C. Zhou¹⁶⁹, H. Zhou⁷, N. Zhou^{62c}, Y. Zhou⁷, C. G. Zhu^{62b}, C. Zhu^{14a,14d}, H. L. Zhu^{62a}, H. Zhu^{14a}, J. Zhu¹⁰⁵, Y. Zhu^{62c}, Y. Zhu^{62a}, X. Zhuang^{14a}, K. Zhukov³⁷, V. Zhulanov³⁷, N. I. Zimine³⁸, J. Zinsser^{63b}, M. Ziolkowski¹⁴⁰, L. Živković¹⁵, A. Zoccoli^{23a,23b}, K. Zoch⁵⁶, T. G. Zorbas¹³⁸, O. Zormpa⁴⁶, W. Zou⁴¹, L. Zwalinski³⁶

¹ Department of Physics, University of Adelaide, Adelaide, Australia

² Department of Physics, University of Alberta, Edmonton, AB, Canada

³ (a) Department of Physics, Ankara University, Ankara, Türkiye; (b) Division of Physics, TOBB University of Economics and Technology, Ankara, Türkiye

⁴ LAPP, Université Savoie Mont Blanc, CNRS/IN2P3, Annecy, France

⁵ APC, Université Paris Cité, CNRS/IN2P3, Paris, France

- ⁶ High Energy Physics Division, Argonne National Laboratory, Argonne, IL, USA
- ⁷ Department of Physics, University of Arizona, Tucson, AZ, USA
- ⁸ Department of Physics, University of Texas at Arlington, Arlington, TX, USA
- ⁹ Physics Department, National and Kapodistrian University of Athens, Athens, Greece
- ¹⁰ Physics Department, National Technical University of Athens, Zografou, Greece
- ¹¹ Department of Physics, University of Texas at Austin, Austin, TX, USA
- ¹² Institute of Physics, Azerbaijan Academy of Sciences, Baku, Azerbaijan
- ¹³ Institut de Física d'Altes Energies (IFAE), Barcelona Institute of Science and Technology, Barcelona, Spain
- ¹⁴ ^(a)Institute of High Energy Physics, Chinese Academy of Sciences, Beijing, China; ^(b)Physics Department, Tsinghua University, Beijing, China; ^(c)Department of Physics, Nanjing University, Nanjing, China; ^(d)University of Chinese Academy of Science (UCAS), Beijing, China
- ¹⁵ Institute of Physics, University of Belgrade, Belgrade, Serbia
- ¹⁶ Department for Physics and Technology, University of Bergen, Bergen, Norway
- ¹⁷ ^(a)Physics Division, Lawrence Berkeley National Laboratory, Berkeley, CA, USA; ^(b)University of California, Berkeley, CA, USA
- ¹⁸ Institut für Physik, Humboldt Universität zu Berlin, Berlin, Germany
- ¹⁹ Albert Einstein Center for Fundamental Physics and Laboratory for High Energy Physics, University of Bern, Bern, Switzerland
- ²⁰ School of Physics and Astronomy, University of Birmingham, Birmingham, UK
- ²¹ ^(a)Department of Physics, Bogazici University, Istanbul, Türkiye; ^(b)Department of Physics Engineering, Gaziantep University, Gaziantep, Türkiye; ^(c)Department of Physics, Istanbul University, Istanbul, Türkiye; ^(d)Istinye University, Sariyer, Istanbul, Türkiye
- ²² ^(a)Facultad de Ciencias y Centro de Investigaciones, Universidad Antonio Nariño, Bogotá, Colombia; ^(b)Departamento de Física, Universidad Nacional de Colombia, Bogotá, Colombia
- ²³ ^(a)Dipartimento di Fisica e Astronomia A. Righi, Università di Bologna, Bologna, Italy; ^(b)INFN Sezione di Bologna, Bologna, Italy
- ²⁴ Physikalisches Institut, Universität Bonn, Bonn, Germany
- ²⁵ Department of Physics, Boston University, Boston, MA, USA
- ²⁶ Department of Physics, Brandeis University, Waltham, MA, USA
- ²⁷ ^(a)Transilvania University of Brasov, Brasov, Romania; ^(b)Horia Hulubei National Institute of Physics and Nuclear Engineering, Bucharest, Romania; ^(c)Department of Physics, Alexandru Ioan Cuza University of Iasi, Iasi, Romania; ^(d)Physics Department, National Institute for Research and Development of Isotopic and Molecular Technologies, Cluj-Napoca, Romania; ^(e)University Politehnica Bucharest, Bucharest, Romania; ^(f)West University in Timisoara, Timisoara, Romania; ^(g)Faculty of Physics, University of Bucharest, Bucharest, Romania
- ²⁸ ^(a)Faculty of Mathematics, Physics and Informatics, Comenius University, Bratislava, Slovakia; ^(b)Department of Subnuclear Physics, Institute of Experimental Physics of the Slovak Academy of Sciences, Kosice, Slovak Republic
- ²⁹ Physics Department, Brookhaven National Laboratory, Upton, NY, USA
- ³⁰ Instituto de Física de Buenos Aires (IFIBA), Departamento de Física, y CONICET, Facultad de Ciencias Exactas y Naturales, Universidad de Buenos Aires, Buenos Aires, Argentina
- ³¹ California State University, Long Beach, CA, USA
- ³² Cavendish Laboratory, University of Cambridge, Cambridge, UK
- ³³ ^(a)Department of Physics, University of Cape Town, Cape Town, South Africa; ^(b)iThemba Labs, Western Cape, South Africa; ^(c)Department of Mechanical Engineering Science, University of Johannesburg, Johannesburg, South Africa; ^(d)National Institute of Physics, University of the Philippines, Diliman, Philippines; ^(e)Department of Physics, University of South Africa, Pretoria, South Africa; ^(f)University of Zululand, KwaDlangezwa, South Africa; ^(g)School of Physics, University of the Witwatersrand, Johannesburg, South Africa
- ³⁴ Department of Physics, Carleton University, Ottawa, ON, Canada
- ³⁵ ^(a)Faculté des Sciences Ain Chock, Réseau Universitaire de Physique des Hautes Energies, Université Hassan II, Casablanca, Morocco; ^(b)Faculté des Sciences, Université Ibn-Tofail, Kénitra, Morocco; ^(c)Faculté des Sciences Semlalia, Université Cadi Ayyad, LPHEA-Marrakech, Morocco; ^(d)LPMR, Faculté des Sciences, Université Mohamed Premier, Oujda, Morocco; ^(e)Faculté des sciences, Université Mohammed V, Rabat, Morocco; ^(f)Institute of Applied Physics, Mohammed VI Polytechnic University, Ben Guerir, Morocco
- ³⁶ CERN, Geneva, Switzerland

- 37 Affiliated with an Institute Covered by a Cooperation Agreement with CERN, Geneva, Switzerland
- 38 Affiliated with an International Laboratory Covered by a Cooperation Agreement with CERN, Geneva, Switzerland
- 39 Enrico Fermi Institute, University of Chicago, Chicago, IL, USA
- 40 LPC, Université Clermont Auvergne, CNRS/IN2P3, Clermont-Ferrand, France
- 41 Nevis Laboratory, Columbia University, Irvington, NY, USA
- 42 Niels Bohr Institute, University of Copenhagen, Copenhagen, Denmark
- 43 ^(a)Dipartimento di Fisica, Università della Calabria, Rende, Italy; ^(b)INFN Gruppo Collegato di Cosenza, Laboratori Nazionali di Frascati, Frascati, Italy
- 44 Physics Department, Southern Methodist University, Dallas, TX, USA
- 45 Physics Department, University of Texas at Dallas, Richardson, TX, USA
- 46 National Centre for Scientific Research “Demokritos”, Agia Paraskevi, Greece
- 47 ^(a)Department of Physics, Stockholm University, Stockholm, Sweden; ^(b)Oskar Klein Centre, Stockholm, Sweden
- 48 Deutsches Elektronen-Synchrotron DESY, Hamburg and Zeuthen, Germany
- 49 Fakultät Physik, Technische Universität Dortmund, Dortmund, Germany
- 50 Institut für Kern- und Teilchenphysik, Technische Universität Dresden, Dresden, Germany
- 51 Department of Physics, Duke University, Durham, NC, USA
- 52 SUPA-School of Physics and Astronomy, University of Edinburgh, Edinburgh, UK
- 53 INFN e Laboratori Nazionali di Frascati, Frascati, Italy
- 54 Physikalisches Institut, Albert-Ludwigs-Universität Freiburg, Freiburg, Germany
- 55 II. Physikalisches Institut, Georg-August-Universität Göttingen, Göttingen, Germany
- 56 Département de Physique Nucléaire et Corpusculaire, Université de Genève, Geneva, Switzerland
- 57 ^(a)Dipartimento di Fisica, Università di Genova, Genoa, Italy; ^(b)INFN Sezione di Genova, Genoa, Italy
- 58 II. Physikalisches Institut, Justus-Liebig-Universität Giessen, Giessen, Germany
- 59 SUPA-School of Physics and Astronomy, University of Glasgow, Glasgow, UK
- 60 LPSC, Université Grenoble Alpes, CNRS/IN2P3, Grenoble INP, Grenoble, France
- 61 Laboratory for Particle Physics and Cosmology, Harvard University, Cambridge, MA, USA
- 62 ^(a)Department of Modern Physics and State Key Laboratory of Particle Detection and Electronics, University of Science and Technology of China, Hefei, China; ^(b)Institute of Frontier and Interdisciplinary Science and Key Laboratory of Particle Physics and Particle Irradiation (MOE), Shandong University, Qingdao, China; ^(c)School of Physics and Astronomy, Shanghai Jiao Tong University, Key Laboratory for Particle Astrophysics and Cosmology (MOE), SKLPPC, Shanghai, China; ^(d)Tsung-Dao Lee Institute, Shanghai, China
- 63 ^(a)Kirchhoff-Institut für Physik, Ruprecht-Karls-Universität Heidelberg, Heidelberg, Germany; ^(b)Physikalisches Institut, Ruprecht-Karls-Universität Heidelberg, Heidelberg, Germany
- 64 ^(a)Department of Physics, Chinese University of Hong Kong, Shatin, N.T., Hong Kong, China; ^(b)Department of Physics, University of Hong Kong, Hong Kong, China; ^(c)Department of Physics and Institute for Advanced Study, Hong Kong University of Science and Technology, Clear Water Bay, Kowloon, Hong Kong, China
- 65 Department of Physics, National Tsing Hua University, Hsinchu, Taiwan
- 66 IJCLab, Université Paris-Saclay, CNRS/IN2P3, 91405 Orsay, France
- 67 Department of Physics, Indiana University, Bloomington, IN, USA
- 68 ^(a)INFN Gruppo Collegato di Udine, Sezione di Trieste, Udine, Italy; ^(b)ICTP, Trieste, Italy; ^(c)Dipartimento Politecnico di Ingegneria e Architettura, Università di Udine, Udine, Italy
- 69 ^(a)INFN Sezione di Lecce, Lecce, Italy; ^(b)Dipartimento di Matematica e Fisica, Università del Salento, Lecce, Italy
- 70 ^(a)INFN Sezione di Milano, Milan, Italy; ^(b)Dipartimento di Fisica, Università di Milano, Milan, Italy
- 71 ^(a)INFN Sezione di Napoli, Naples, Italy; ^(b)Dipartimento di Fisica, Università di Napoli, Naples, Italy
- 72 ^(a)INFN Sezione di Pavia, Pavia, Italy; ^(b)Dipartimento di Fisica, Università di Pavia, Pavia, Italy
- 73 ^(a)INFN Sezione di Pisa, Pisa, Italy; ^(b)Dipartimento di Fisica E. Fermi, Università di Pisa, Pisa, Italy
- 74 ^(a)INFN Sezione di Roma, Rome, Italy; ^(b)Dipartimento di Fisica, Sapienza Università di Roma, Rome, Italy
- 75 ^(a)INFN Sezione di Roma Tor Vergata, Rome, Italy; ^(b)Dipartimento di Fisica, Università di Roma Tor Vergata, Rome, Italy
- 76 ^(a)INFN Sezione di Roma Tre, Rome, Italy; ^(b)Dipartimento di Matematica e Fisica, Università Roma Tre, Rome, Italy
- 77 ^(a)INFN-TIFPA, Povo, Italy; ^(b)Università degli Studi di Trento, Trento, Italy
- 78 Department of Astro and Particle Physics, Universität Innsbruck, Innsbruck, Austria
- 79 University of Iowa, Iowa City, IA, USA

- ⁸⁰ Department of Physics and Astronomy, Iowa State University, Ames, IA, USA
- ⁸¹ ^(a)Departamento de Engenharia Elétrica, Universidade Federal de Juiz de Fora (UFJF), Juiz de Fora, Brazil ; ^(b)Universidade Federal do Rio de Janeiro COPPE/EE/IF, Rio de Janeiro, Brazil; ^(c)Instituto de Física, Universidade de São Paulo, São Paulo, Brazil; ^(d)Rio de Janeiro State University, Rio de Janeiro, Brazil
- ⁸² KEK, High Energy Accelerator Research Organization, Tsukuba, Japan
- ⁸³ Graduate School of Science, Kobe University, Kobe, Japan
- ⁸⁴ ^(a)Faculty of Physics and Applied Computer Science, AGH University of Krakow, Krakow, Poland; ^(b)Marian Smoluchowski Institute of Physics, Jagiellonian University, Krakow, Poland
- ⁸⁵ Institute of Nuclear Physics Polish Academy of Sciences, Krakow, Poland
- ⁸⁶ Faculty of Science, Kyoto University, Kyoto, Japan
- ⁸⁷ Kyoto University of Education, Kyoto, Japan
- ⁸⁸ Research Center for Advanced Particle Physics and Department of Physics, Kyushu University, Fukuoka, Japan
- ⁸⁹ Instituto de Física La Plata, Universidad Nacional de La Plata and CONICET, La Plata, Argentina
- ⁹⁰ Physics Department, Lancaster University, Lancaster, UK
- ⁹¹ Oliver Lodge Laboratory, University of Liverpool, Liverpool, UK
- ⁹² Department of Experimental Particle Physics, Jožef Stefan Institute and Department of Physics, University of Ljubljana, Ljubljana, Slovenia
- ⁹³ School of Physics and Astronomy, Queen Mary University of London, London, UK
- ⁹⁴ Department of Physics, Royal Holloway University of London, Egham, UK
- ⁹⁵ Department of Physics and Astronomy, University College London, London, UK
- ⁹⁶ Louisiana Tech University, Ruston, LA, USA
- ⁹⁷ Fysiska institutionen, Lunds universitet, Lund, Sweden
- ⁹⁸ Departamento de Física Teórica C-15 and CIAFF, Universidad Autónoma de Madrid, Madrid, Spain
- ⁹⁹ Institut für Physik, Universität Mainz, Mainz, Germany
- ¹⁰⁰ School of Physics and Astronomy, University of Manchester, Manchester, UK
- ¹⁰¹ CPPM, Aix-Marseille Université, CNRS/IN2P3, Marseille, France
- ¹⁰² Department of Physics, University of Massachusetts, Amherst, MA, USA
- ¹⁰³ Department of Physics, McGill University, Montreal, QC, Canada
- ¹⁰⁴ School of Physics, University of Melbourne, Victoria, Australia
- ¹⁰⁵ Department of Physics, University of Michigan, Ann Arbor, MI, USA
- ¹⁰⁶ Department of Physics and Astronomy, Michigan State University, East Lansing, MI, USA
- ¹⁰⁷ Group of Particle Physics, University of Montreal, Montreal, QC, Canada
- ¹⁰⁸ Fakultät für Physik, Ludwig-Maximilians-Universität München, Munich, Germany
- ¹⁰⁹ Max-Planck-Institut für Physik (Werner-Heisenberg-Institut), Munich, Germany
- ¹¹⁰ Graduate School of Science and Kobayashi-Maskawa Institute, Nagoya University, Nagoya, Japan
- ¹¹¹ Department of Physics and Astronomy, University of New Mexico, Albuquerque, NM, USA
- ¹¹² Institute for Mathematics, Astrophysics and Particle Physics, Radboud University/Nikhef, Nijmegen, The Netherlands
- ¹¹³ Nikhef National Institute for Subatomic Physics and University of Amsterdam, Amsterdam, The Netherlands
- ¹¹⁴ Department of Physics, Northern Illinois University, DeKalb, IL, USA
- ¹¹⁵ ^(a)New York University Abu Dhabi, Abu Dhabi, United Arab Emirates; ^(b)University of Sharjah, Sharjah, United Arab Emirates
- ¹¹⁶ Department of Physics, New York University, New York, NY, USA
- ¹¹⁷ Ochanomizu University, Otsuka, Bunkyo-ku, Tokyo, Japan
- ¹¹⁸ Ohio State University, Columbus, OH, USA
- ¹¹⁹ Homer L. Dodge Department of Physics and Astronomy, University of Oklahoma, Norman, OK, USA
- ¹²⁰ Department of Physics, Oklahoma State University, Stillwater, OK, USA
- ¹²¹ Palacký University, Joint Laboratory of Optics, Olomouc, Czech Republic
- ¹²² Institute for Fundamental Science, University of Oregon, Eugene, OR, USA
- ¹²³ Graduate School of Science, Osaka University, Osaka, Japan
- ¹²⁴ Department of Physics, University of Oslo, Oslo, Norway
- ¹²⁵ Department of Physics, Oxford University, Oxford, UK
- ¹²⁶ LPNHE, Sorbonne Université, Université Paris Cité, CNRS/IN2P3, Paris, France
- ¹²⁷ Department of Physics, University of Pennsylvania, Philadelphia, PA, USA

- 128 Department of Physics and Astronomy, University of Pittsburgh, Pittsburgh, PA, USA
- 129 (a) Laboratório de Instrumentação e Física Experimental de Partículas-LIP, Lisbon, Portugal; (b) Departamento de Física, Faculdade de Ciências, Universidade de Lisboa, Lisbon, Portugal; (c) Departamento de Física, Universidade de Coimbra, Coimbra, Portugal; (d) Centro de Física Nuclear da Universidade de Lisboa, Lisbon, Portugal; (e) Departamento de Física, Universidade do Minho, Braga, Portugal; (f) Departamento de Física Teórica y del Cosmos, Universidad de Granada, Granada, Spain; (g) Departamento de Física, Instituto Superior Técnico, Universidade de Lisboa, Lisbon, Portugal
- 130 Institute of Physics of the Czech Academy of Sciences, Prague, Czech Republic
- 131 Czech Technical University in Prague, Prague, Czech Republic
- 132 Faculty of Mathematics and Physics, Charles University, Prague, Czech Republic
- 133 Particle Physics Department, Rutherford Appleton Laboratory, Didcot, UK
- 134 IRFU, CEA, Université Paris-Saclay, Gif-sur-Yvette, France
- 135 Santa Cruz Institute for Particle Physics, University of California Santa Cruz, Santa Cruz, CA, USA
- 136 (a) Departamento de Física, Pontificia Universidad Católica de Chile, Santiago, Chile; (b) Millennium Institute for Subatomic physics at high energy frontier (SAPHIR), Santiago, Chile; (c) Instituto de Investigación Multidisciplinario en Ciencia y Tecnología y Departamento de Física, Universidad de La Serena, La Serena, Chile; (d) Department of Physics, Universidad Andres Bello, Santiago, Chile; (e) Instituto de Alta Investigación, Universidad de Tarapacá, Arica, Chile; (f) Departamento de Física, Universidad Técnica Federico Santa María, Valparaíso, Chile
- 137 Department of Physics, University of Washington, Seattle, WA, USA
- 138 Department of Physics and Astronomy, University of Sheffield, Sheffield, UK
- 139 Department of Physics, Shinshu University, Nagano, Japan
- 140 Department Physik, Universität Siegen, Siegen, Germany
- 141 Department of Physics, Simon Fraser University, Burnaby, BC, Canada
- 142 SLAC National Accelerator Laboratory, Stanford, CA, USA
- 143 Department of Physics, Royal Institute of Technology, Stockholm, Sweden
- 144 Departments of Physics and Astronomy, Stony Brook University, Stony Brook, NY, USA
- 145 Department of Physics and Astronomy, University of Sussex, Brighton, UK
- 146 School of Physics, University of Sydney, Sydney, Australia
- 147 Institute of Physics, Academia Sinica, Taipei, Taiwan
- 148 (a) E. Andronikashvili Institute of Physics, Iv. Javakhishvili Tbilisi State University, Tbilisi, Georgia; (b) High Energy Physics Institute, Tbilisi State University, Tbilisi, Georgia; (c) University of Georgia, Tbilisi, Georgia
- 149 Department of Physics, Technion, Israel Institute of Technology, Haifa, Israel
- 150 Raymond and Beverly Sackler School of Physics and Astronomy, Tel Aviv University, Tel Aviv, Israel
- 151 Department of Physics, Aristotle University of Thessaloniki, Thessaloniki, Greece
- 152 International Center for Elementary Particle Physics and Department of Physics, University of Tokyo, Tokyo, Japan
- 153 Department of Physics, Tokyo Institute of Technology, Tokyo, Japan
- 154 Department of Physics, University of Toronto, Toronto, ON, Canada
- 155 (a) TRIUMF, Vancouver, BC, Canada; (b) Department of Physics and Astronomy, York University, Toronto, ON, Canada
- 156 Division of Physics and Tomonaga Center for the History of the Universe, Faculty of Pure and Applied Sciences, University of Tsukuba, Tsukuba, Japan
- 157 Department of Physics and Astronomy, Tufts University, Medford, MA, USA
- 158 United Arab Emirates University, Al Ain, United Arab Emirates
- 159 Department of Physics and Astronomy, University of California Irvine, Irvine, CA, USA
- 160 Department of Physics and Astronomy, University of Uppsala, Uppsala, Sweden
- 161 Department of Physics, University of Illinois, Urbana, IL, USA
- 162 Instituto de Física Corpuscular (IFIC), Centro Mixto Universidad de Valencia-CSIC, Valencia, Spain
- 163 Department of Physics, University of British Columbia, Vancouver, BC, Canada
- 164 Department of Physics and Astronomy, University of Victoria, Victoria, BC, Canada
- 165 Fakultät für Physik und Astronomie, Julius-Maximilians-Universität Würzburg, Würzburg, Germany
- 166 Department of Physics, University of Warwick, Coventry, UK
- 167 Waseda University, Tokyo, Japan
- 168 Department of Particle Physics and Astrophysics, Weizmann Institute of Science, Rehovot, Israel
- 169 Department of Physics, University of Wisconsin, Madison, WI, USA

- ¹⁷⁰ Fakultät für Mathematik und Naturwissenschaften, Fachgruppe Physik, Bergische Universität Wuppertal, Wuppertal, Germany
- ¹⁷¹ Department of Physics, Yale University, New Haven, CT, USA
- ^a Also Affiliated with an Institute Covered by a Cooperation Agreement with CERN, Geneva, Switzerland
- ^b Also at An-Najah National University, Nablus, Palestine
- ^c Also at Borough of Manhattan Community College, City University of New York, New York, NY, USA
- ^d Also at Bruno Kessler Foundation, Trento, Italy
- ^e Also at Center for High Energy Physics, Peking University, Beijing, China
- ^f Also at Center for Interdisciplinary Research and Innovation (CIRI-AUTH), Thessaloniki, Greece
- ^g Also at Centro Studi e Ricerche Enrico Fermi, Rome, Italy
- ^h Also at CERN, Geneva, Switzerland
- ⁱ Also at Département de Physique Nucléaire et Corpusculaire, Université de Genève, Geneva, Switzerland
- ^j Also at Departament de Física de la Universitat Autònoma de Barcelona, Barcelona, Spain
- ^k Also at Department of Financial and Management Engineering, University of the Aegean, Chios, Greece
- ^l Also at Department of Physics and Astronomy, Michigan State University, East Lansing, MI, USA
- ^m Also at Department of Physics and Astronomy, University of Louisville, Louisville, KY, USA
- ⁿ Also at Department of Physics, Ben Gurion University of the Negev, Beer Sheva, Israel
- ^o Also at Department of Physics, California State University, East Bay, USA
- ^p Also at Department of Physics, California State University, Sacramento, USA
- ^q Also at Department of Physics, King's College London, London, UK
- ^r Also at Department of Physics, Stanford University, Stanford, CA, USA
- ^s Also at Department of Physics, University of Fribourg, Fribourg, Switzerland
- ^t Also at Department of Physics, University of Thessaly, Thessaly, Greece
- ^u Also at Department of Physics, Westmont College, Santa Barbara, USA
- ^v Also at Hellenic Open University, Patras, Greece
- ^w Also at Institutio Catalana de Recerca i Estudis Avancats, ICREA, Barcelona, Spain
- ^x Also at Institut für Experimentalphysik, Universität Hamburg, Hamburg, Germany
- ^y Also at Institute for Nuclear Research and Nuclear Energy (INRNE) of the Bulgarian Academy of Sciences, Sofia, Bulgaria
- ^z Also at Institute of Particle Physics (IPP), Victoria, Canada
- ^{aa} Also at Institute of Physics and Technology, Ulaanbaatar, Mongolia
- ^{ab} Also at Institute of Physics, Azerbaijan Academy of Sciences, Baku, Azerbaijan
- ^{ac} Also at Institute of Theoretical Physics, Ilia State University, Tbilisi, Georgia
- ^{ad} Also at L2IT, Université de Toulouse, CNRS/IN2P3, UPS, Toulouse, France
- ^{ae} Also at Lawrence Livermore National Laboratory, Livermore, USA
- ^{af} Also at National Institute of Physics, University of the Philippines, Diliman, Philippines
- ^{ag} Also at III. Physikalisches Institut A, RWTH Aachen University, Aachen, Germany
- ^{ah} Also at Technical University of Munich, Munich, Germany
- ^{ai} Also at The Collaborative Innovation Center of Quantum Matter (CICQM), Beijing, China
- ^{aj} Also at TRIUMF, Vancouver, BC, Canada
- ^{ak} Also at Università di Napoli Parthenope, Naples, Italy
- ^{al} Also at University of Chinese Academy of Sciences (UCAS), Beijing, China
- ^{am} Also at Department of Physics, University of Colorado Boulder, Colorado, USA
- ^{an} Also at Washington College, Chestertown, MD, USA
- ^{ao} Also at Physics Department, Yeditepe University, Istanbul, Türkiye
- * Deceased